

DUDLEY KNOX LIBRARY
NAVAL POSTGRADUATE SCHOOL
MONTEREY CA 93943-5101

NAVAL POSTGRADUATE SCHOOL

Monterey , California



THESIS

NUMERICAL STUDIES OF THE BETA-EFFECT IN
TROPICAL CYCLONE
MOTION USING A SEMI-LAGRANGIAN MODEL

by

TeriAnn Lentz

December 1991

Thesis Advisor

R. T. Williams

Approved for public release; distribution is unlimited.

REPORT DOCUMENTATION PAGE

1a Report Security Classification Unclassified			1b Restrictive Markings		
2a Security Classification Authority			3 Distribution/Availability of Report		
2b Declassification Downgrading Schedule			Approved for public release; distribution is unlimited.		
4 Performing Organization Report Number(s)			5 Monitoring Organization Report Number(s)		
6a Name of Performing Organization Naval Postgraduate School		6b Office Symbol (if applicable) 35	7a Name of Monitoring Organization Naval Postgraduate School		
6c Address (city, state, and ZIP code) Monterey, CA 93943-5000			7b Address (city, state, and ZIP code) Monterey, CA 93943-5000		
8a Name of Funding, Sponsoring Organization		8b Office Symbol (if applicable)	9 Procurement Instrument Identification Number		
8c Address (city, state, and ZIP code)			10 Source of Funding Numbers		
			Program Element No	Project No	Task No
			Work Unit Accession No		
11 Title (include security classification) NUMERICAL STUDIES OF THE BETA-EFFECT IN TROPICAL CYCLONE MOTION USING A SEMI-LAGRANGIAN MODEL					
12 Personal Author(s) TeriAnn Lentz					
13a Type of Report Master's Thesis		13b Time Covered From To		14 Date of Report (year, month, day) December 1991	
				15 Page Count 50	
16 Supplementary Notation The views expressed in this thesis are those of the author and do not reflect the official policy or position of the Department of Defense or the U.S. Government.					
17 Cosati Codes			18 Subject Terms (continue on reverse if necessary and identify by block number)		
Field	Group	Subgroup	Numerical Modeling, Semi-Lagrangian Theory, Beta Drift		
19 Abstract (continue on reverse if necessary and identify by block number) It has been found that the beta effect can have an important effect on tropical cyclones. To conduct an experimental study of tropical cyclone movement on a beta plane a numerical model was developed. This model is based on the barotropic vorticity equation and used a semi-Lagrangian technique for the advective terms. The basic model is studied for accuracy and efficiency. It is seen that the accuracy of the semi-Lagrangian scheme is very good at moderate grid intervals, 20 km to 40 km, producing a much smoother vorticity field than that produced by the finite difference model. The efficiency of the semi-Lagrangian scheme as the time interval was increased was not fully achieved due to the shear effect in this regional model. When the beta effect was added, the model predicted vortex tracks and beta gyres compared well with those obtained from the finite difference model with a 20 km grid size. However, the semi-Lagrangian forecast with a grid size of 10 km gave somewhat different track, which could not be explained.					
20 Distribution Availability of Abstract <input checked="" type="checkbox"/> unclassified unlimited <input type="checkbox"/> same as report <input type="checkbox"/> DTIC users				21 Abstract Security Classification Unclassified	
22a Name of Responsible Individual R. T. Williams		22b Telephone (include Area code) (408) 646-2296		22c Office Symbol MR/Wu	

Approved for public release; distribution is unlimited.

Numerical Studies of the Beta-Effect in Tropical Cyclone
Motion using a Semi-Lagrangian Model

by

TeriAnn Lentz
Lieutenant , United States Navy
B.S. Meteorology, University of Wisconsin, 1981

Submitted in partial fulfillment of the
requirements for the degree of

MASTER OF SCIENCE IN METEOROLOGY AND PHYSICAL
OCEANOGRAPHY

from the

NAVAL POSTGRADUATE SCHOOL
December 1991

ABSTRACT

It has been found that the beta effect can have an important effect on tropical cyclones. To conduct an experimental study of tropical cyclone movement on a beta plane a numerical model was developed. This model is based on the barotropic vorticity equation and used a semi-Lagrangian technique for the advective terms. The basic model is studied for accuracy and efficiency. It is seen that the accuracy of the semi-Lagrangian scheme is very good at moderate grid intervals, 20 km to 40 km, producing a much smoother vorticity field than that produced by the finite difference model. The efficiency of the semi-Lagrangian scheme as the time interval was increased was not fully achieved due to the shear effect in this regional model. When the beta effect was added, the model predicted vortex tracks and beta gyres compared well with those obtained from the finite difference model with a 20 km grid size. However, the semi-Lagrangian forecast with a grid size of 10 km gave somewhat different track, which could not be explained.

TABLE OF CONTENTS

I. INTRODUCTION	1
II. MODEL DEVELOPMENT	5
A. GENERAL FORMULATION:	5
B. SEMI-LAGRANGIAN METHOD	7
C. INTERPOLATION	8
III. ACCURACY OF THE SEMI-LAGRANGIAN MODEL	9
A. BASIC COMPARISON	9
B. TIME STEP VARIATIONS	10
C. GRID SIZE VARIATIONS	12
D. SUMMARY	14
IV. BETA DRIFT AND MODEL ACCURACY	21
A. NO MEAN FLOW EXPERIMENTS	21
1. Basic Comparison	21
2. Time Step Variations	22
3. Grid Size Variations	24
B. ASYMMETRIC CIRCULATIONS	25
C. SUMMARY	26
V. CONCLUSION	37
VI. RECOMMENDATIONS	39
REFERENCES	40
INITIAL DISTRIBUTION LIST	42

LIST OF TABLES

Table 1.	AVERAGE FORECAST ERRORS FOR 1990 TYPHOON SEASON . . .	1
Table 2.	MAGNITUDE OF VORTEX FOR DIFFERENT ITERATIONS OF MODEL	12
Table 3.	MAGNITUDE OF VORTEX WHEN VARYING DISPLACEMENT ACCURACY	13
Table 4.	TRACK COMPARISON SEMI-LAGRANGIAN/FINITE DIFFERENCE	23

LIST OF FIGURES

Figure 1.	Upstream Scheme	3
Figure 2.	Basic Comparison Forecast Tracks	9
Figure 3.	Basic Comparison Forecast	15
Figure 4.	Varied Error Restrictions Forecast	16
Figure 5.	Varied Error Restriction Forecast Tracks	17
Figure 6.	Grid Size Variation Comparison Forecast Tracks	18
Figure 7.	Grid Size Variation Comparison Forecast	19
Figure 8.	Error Restriction Test	20
Figure 9.	Semi-Lagrangian Forecast on a Beta Plane	27
Figure 10.	Basic Comparison Forecast Tracks with Beta	28
Figure 11.	Semi-Lagrangian Forecast on a Beta Plane	29
Figure 12.	Semi-Lagrangian Forecast Tracks with Beta	30
Figure 13.	Grid Size Variation Forecast with Beta	31
Figure 14.	Grid Size Variation Forecast Tracks with Beta	32
Figure 15.	Grid Size Variation Forecast Track with Beta	33
Figure 16.	Wave Number One Gyre	34
Figure 17.	Wave Number One Amplitude Growth	35
Figure 18.	Wave Number One Amplitude Comparison	36

I. INTRODUCTION

In December 1944, the U.S. Third Fleet lost 778 officers and men, three ships and over 140 aircraft to a typhoon in the Phillipine Sea. While many factors contributed to the fleets entrapment, the most significant were failures in command and lack of quality weather warning capabilities and observational facilities (Calhoun, 1981).

Since 1944, great strides have been made in determining the position and intensity of a tropical cyclone through the use of an improved observation network and satellites. Through the development of computers and numerical models, improvements have also been made in our ability to forecast the cyclone's movement. In 1990, forecast errors reported by the Joint Typhoon Warning Center for the Western Pacific are given in Table 1.

Table 1. AVERAGE FORECAST ERRORS FOR 1990 TYPHOON SEASON

Forecast Verifying Time	24 hrs	48 hrs	72 hrs
	103NM	203NM	310NM

In 1982, Commander U. S. Seventh Fleet declared that he wanted to reduce the forecast error statistics by approximately 60 percent at each forecast period (EGPACCOM, 1983). As the error rate in 1990 shows little improvement over 1982, to meet the goals as set down by COMSEVENTHFLT, continued efforts must be made in improving our ability to forecast the movement of tropical cyclones.

Forecasting a tropical cyclone's movement is a difficult problem as it depends upon the interaction between many factors and usually occurs over a data sparse, mainly oceanic area. After Nuemann (1985), objective tropical cyclone prediction aids can be classified as either dynamical or statistical. These categories are divided further into six subdivisions. Statistical models are divided into analog, climatological/persistence, and statistical/synoptic. Dynamical models can be a blend of basic dynamics and statistics, barotropic, or baroclinic. The statistical forecast approach commonly uses a screening procedure to select meteorological variables that are correlated with tropical cyclone movement. The dynamical method involves predictions of the synoptic flow surrounding a tropical cyclone and possibly a simulation of the cyclone structure to predict storm

movement. (George and Gray, 1976). Tsui and Miller (1988) showed through their research that while dynamical models have properties that make them the better choice for a forecast aid, as of yet no one type of forecast model is better in all cases. A major problem facing many developers of dynamical models is the amount of available computing power. With today's technology, super computers are at least eight times faster than those of just ten years ago. Though while computers may be faster in the speed in which calculations are done, the modeler must also develop software to enhance the speed of the hardware.

Numerous studies on different numerical schemes have been done to date. Some of these studies have been implemented into objective aids to use in forecasting tropical cyclones. But despite many advances made in the field of computational fluid dynamics, the advective terms are still an active area of research (Pudykiewicz and Staniforth, 1984). One scheme that has seen renewed interest is the semi-Lagrangian method for handling advection in meteorological models. Semi-Lagrangian schemes are not new. Sawyer (1963) proposed solving the vorticity advection equation with the semi-Lagrangian scheme. Robert (1981) used a variation of the semi-Lagrangian scheme to solve the primitive meteorological equations. In 1984, Pudykiewicz and Staniforth researched the schemes use in the solution of the advection-diffusion equation relating it to pollution models. Staniforth and Templeton (1986) used the semi-Lagrangian scheme in their research with a barotropic finite element model. Kuo and Williams (1989) applied the scheme to the Inviscid Burgers Equation showing that at sharp slopes the method is superior to finite difference schemes. At this time, Florida State University is using a version of the semi-Lagrangian method in a multi-layered regional model for the tropics.

A lagrangian method is based on the simple fact that what happens at a future time at a point is related to what happened at a point upstream at an earlier time. One of the simplest Lagrangian schemes is the upstream scheme which is described in the following discussion. Figure 1 on page 3 shows the characteristic which passes through the point $P(m,n+1)$ at which we want to predict the function F . The advective flow is given by c . Since the function F is constant along the characteristic then

$$F_p = F(m\Delta x, (n+1)\Delta t) = F(m\Delta x - \delta x, n\Delta t) \quad (1.1)$$

where $\delta x = c\Delta t$ is the distance an air parcel moves. A linear interpolation scheme is used to find the value at * point. In general, the stability of the scheme is described by

$c \geq 0$: damped or neutral solutions provided the CFL condition $0 \leq c \frac{\Delta t}{\Delta x} \leq 1$ is met.

$c < 0$: solutions are amplified or conditionally unstable.

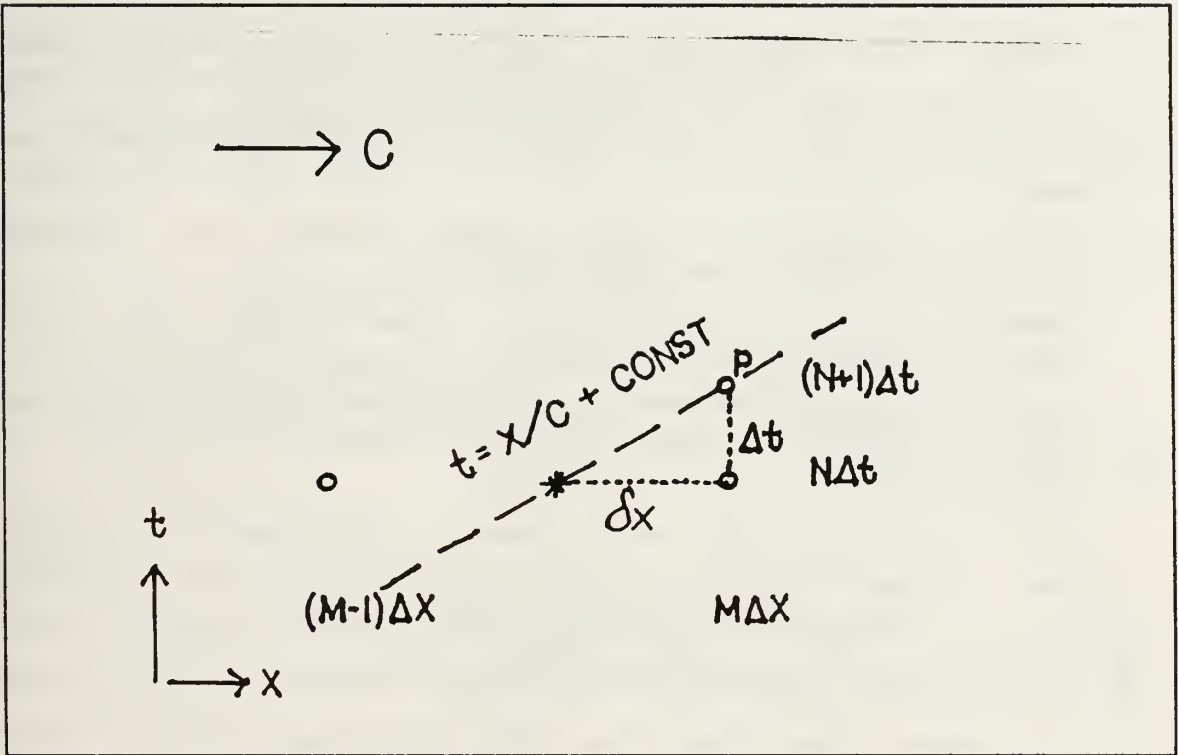


Figure 1. Upstream Scheme

This simple Lagrangian method has some excellent properties such as smoothness of forecast and good phase speed, but it also has too much damping and the time step must satisfy a restrictive CFL condition. The semi-Lagrangian schemes use higher order interpolation routines in space to avoid the problem of damping. They also use an implicit approach to allow for larger time steps and guarantee stability under all CFL conditions.

According to Pudykiewicz & Staniforth (1984), the attractive qualities of the semi-Lagrangian method that lead one to believe that this method has considerable promise for handling meteorological problems include:

1. The method is unconditionally stable for increasing time steps.
2. The method is an efficient time integration scheme.

3. The method gives smaller phase errors and computational dispersion than most finite difference or finite element schemes.
4. The method is accurate for a broad range of flows including those with strong deformation.
5. The method is flexible allowing for variable resolutions and easy handling of out-flow situations at boundaries without spurious reflection.

The primary goal of this thesis is to examine how the semi-Lagrangian method based on Robert's work (1981) relates the movement of tropical cyclones to the advective processes evident in a regional model. Specifically, the objectives can be stated as follows:

1. Develop semi-Lagrangian numerical model which solves the nondivergent barotropic vorticity equation.
2. Determine if the semi-Lagrangian scheme is practical on a large scale in comparison to a standard finite difference scheme.
3. Examine movement of the vortex on a β -plane without mean flow and verify northwestward drift as analyzed in Chan and Williams (1987) and Fiorino and Elsberry (1988).

The nondivergent barotropic model developed for this research is discussed in Chapter II. Chapter III discusses experiments with the basic model without considering the Beta term. Experiments which include the effects of Beta are analyzed in Chapter IV. Conclusions and recommendations are contained in Chapter V and VI respectively.

II. MODEL DEVELOPMENT

A. GENERAL FORMULATION:

The basis of this thesis is a model developed by Tupaz(1977) and modified by Chan and Williams (1987) to study applications of the barotropic vorticity equation. The basic model development is taken directly from Tupaz (1977).

The governing equations are the barotropic vorticity equation using a beta(β) plane approximation

$$\frac{\partial \zeta}{\partial t} + u \frac{\partial \zeta}{\partial x} + v \frac{\partial \zeta}{\partial y} + \beta v = 0 \quad (2.1)$$

and the non-divergent continuity equation

$$\frac{\partial u}{\partial x} + \frac{\partial v}{\partial y} = 0 \quad (2.2)$$

where

$$\zeta \equiv \frac{\partial v}{\partial x} - \frac{\partial u}{\partial y} \quad (2.3)$$

Here β is the north - south gradient of the earth's vorticity and it is given by its value at 10 degrees latitude. Friction and other forcing terms are not considered in this model. Since the flow is two dimensional and non-divergent, the vorticity field can be represented by the streamfunction (Ψ) defined as

$$u = - \frac{\partial \Psi}{\partial y}, \quad v = \frac{\partial \Psi}{\partial x} \quad (2.4)$$

where u and v are the velocities of the flow in the x and y direction, respectively. Thus the relative vorticity is

$$\zeta = \nabla^2 \Psi \quad (2.5)$$

Equation (2.1) now becomes

$$\frac{\partial \nabla^2 \Psi}{\partial t} - \frac{\partial \Psi}{\partial y} \frac{\partial \nabla^2 \Psi}{\partial x} + \frac{\partial \Psi}{\partial x} \frac{\partial \nabla^2 \Psi}{\partial y} + \beta \frac{\partial \Psi}{\partial x} = 0 \quad (2.6)$$

The mean flow is initialized as the basic state streamfunction over a domain defined as an east-west channel with cyclic boundary conditions in the zonal direction. At the north-south boundaries the mean streamfunction is

$$\overline{\Psi}_{i,j} = 0 \quad \text{at } j = 0, j = J \quad (2.7)$$

and

$$\overline{\Psi}_{i,J-1} = \overline{\Psi}_{i,J-2}, \overline{\Psi}_{i,J+1} = \overline{\Psi}_{i,J+2} \quad (2.8)$$

where the meridional domain is defined by

$$0 \leq j \leq J \quad (2.9)$$

Here $x = i\Delta x$ and $y = j\Delta y$. The mean flow used in this study is constant and from the east. As in Chan and Williams (1987), a vortex is entered into the main flow as the perturbation quantity of relative vorticity (ζ'). A cyclonic vortex with a tangential wind $V(r)$ profile of

$$V(r) = V_m \left(\frac{r}{r_m} \right) \exp \left[\frac{1}{b} \left\{ 1 - \left(\frac{r}{r_m} \right)^b \right\} \right] \quad (2.10)$$

is used in this study. The radius is defined as r . V_m is the value of $V(r)$ at the radius of maximum wind r_m and b is a factor that determines the shape of the vortex. Thus the vorticity profile is given by

$$\zeta(r) = \frac{2V_m}{r_m} \left\{ 1 - \frac{1}{2} \left(\frac{r}{r_m} \right)^b \right\} \exp \left[\frac{1}{b} \left\{ 1 - \left(\frac{r}{r_m} \right)^b \right\} \right] \quad (2.11)$$

To handle the advection terms the semi-Lagrangian scheme based on an algorithm of Robert (1981) is used to replace the finite difference scheme used by Tupaz (1977). Relative vorticity is predicted during successive time steps. Equation 2.5 is then solved for the streamfunction to determine the subsequent wind components used in the advection scheme.

Equation 2.5 is a Poisson Equation with the streamfunction as the dependent variable and relative vorticity is the forcing term. The Poisson Equation is solved for the streamfunction with a direct method developed by Sweet (1971). This method uses a finite difference approximation to Poisson's Equation on a rectangular domain with

Dirichlet Boundary Conditions; matrix is inverted directly. The the boundary conditions are as follows:

a. Northern ($j = J$) and Southern ($j = 0$) Boundaries:

$$\Psi'_{i,J} = 0: i = 0, 1, 2, \dots, I \quad (2.12)$$

$$\Psi'_{i,0} = 0: i = 0, 1, 2, \dots, I \quad (2.13)$$

b) Eastern ($i = I$) and Western ($i = 0$) boundaries: These boundaries are periodic where

$$\Psi'_{1,J} = \Psi'_{I-1,J} \quad (2.14)$$

and

$$\Psi'_{2,J} = \Psi'_{I,J} \quad (2.15)$$

Further details on the method used to solve the Poisson Equation can be found in Tupaz (1977).

B. SEMI-LAGRANGIAN METHOD

In this study, we defined a regular mesh of M by M points where (x, y) is defined to be a point of the mesh. At each mesh point, we know ζ , u and v at time t . Equation 2.1 is rewritten by the following approximate equations:

$$\zeta(x, y, t + \Delta t) = \zeta(x - 2a, y - 2b, t - \Delta t) - 2b\beta \quad (2.16)$$

$$a = \Delta t u(x - a, y - b, t) \quad (2.17)$$

$$b = \Delta t v(x - a, y - b, t) \quad (2.18)$$

The following algorithm modeled after Robert (1981) and Pudykiewicz and Staniforth (1984) provides a solution to the vorticity equation by the semi-Lagrangian method.

1. Solve equations 2.17 and 2.18 iteratively for a and b displacements in x and y , respectively. An interpolation formula is used to evaluate u and v between mesh points.
2. Use an interpolation formula to obtain upstream values of ζ .
3. Add in term pertaining to the earth's vorticity ($-2b\beta$)
4. Repeat steps 1 to 3.

In step one, an iterative routine is required because a and b appear on both sides of equation 2.17 and 2.18. Approximate values of a and b are used to evaluate the right-hand side of the equation. In this study, we used a and b at the previous time step as the first guess. The iteration technique is assumed to converge quickly to a more accurate value. Robert (1981) showed that after two iterations the differences were quite small. In Pudykiewicz and Staniforth (1984) the fixed point theorem of Conte and Deboor (1972) was used to assure convergence of the iteration technique. In this study, an error value of 1.0×10^{-5} , which equates to an error of ten meters, controlled the number of iterations. Decreasing this error value increased the number of iterations, cost more in computing efforts, and did not significantly improve the forecast ability of the model.

In step three, we considered

$$\zeta(x,y,t+\Delta t)+f(y,t+\Delta t)=\zeta(x-2a,y-2b,t-\Delta t)+f(y-2b,t-\Delta t) \quad (2.19)$$

recombining equation 2.19

$$\zeta(x,y,t+\Delta t)=\zeta(x-2a,y-2b,t-\Delta t)+f(y-2b,t-\Delta t)-f(y,t+\Delta t) \quad (2.20)$$

If we use the beta approximation and let $f=f_o+\beta_\alpha y$, then equation 2.20 simplifies to equation 2.16.

C. INTERPOLATION

Interpolation by bicubic splines was chosen for this research. During interpolation, the Beta term was set to zero. The interpolation code used was taken and modified from Prof.M. Peng. The method of bicubic splines consisted in fitting the following curve

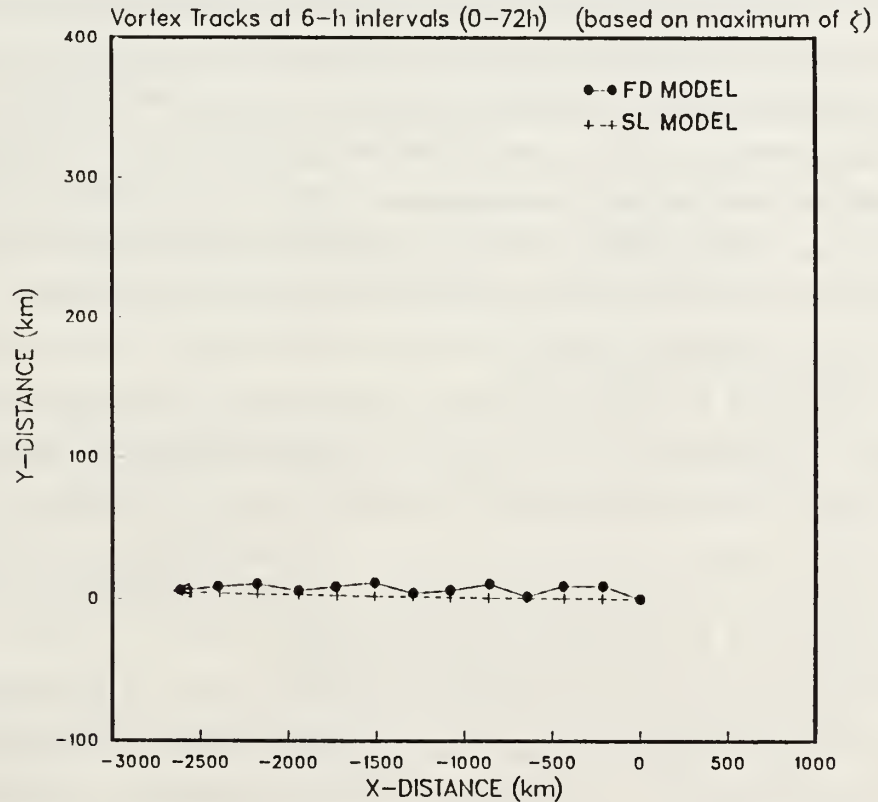
$$F(x,y)=\sum_{m=0}^3\sum_{n=0}^3C_{mn}(x-x_i)(y-y_j) \quad (2.21)$$

to 16 coefficients of a four point square in which the desired point sought is located within the four point square. East - west boundary conditions again were set to be periodic to keep the vortex within the channel. If an upstream point was located outside the grid on the north or south boundaries the value calculated at the nearest boundary was used.

III. ACCURACY OF THE SEMI-LAGRANGIAN MODEL

A. BASIC COMPARISON

In this chapter, results are presented from various iterations of the developed semi-Lagrangian model. In these experiments, the effects of beta were not included. In the first experiment, we compared the semi-Lagrangian model with the finite difference model used in Chan and Williams (1987). The finite difference model with a time step of six minutes and a spatial separation of 20 km was used as the control forecast. With the movement of the vorticity maximum, both models were comparable maintaining constant speed. Figure 2 though shows that the semi-Lagrangian forecast maintained a smoother track in regards to direction than that of the finite difference model.



$$r_{\text{mov}} = 100. \text{ km} \quad v_{\text{mov}} = 40. \text{ m s}^{-1} \quad b = 1.$$

Figure 2. Basic Comparison Forecast Tracks: Finite Difference and Semi-Lagrangian Models both run with the Time step = 6 min and Grid interval = 20 KM

The smoothness of the track may be due to semi-Lagrangian scheme, or more directly related to the damping from the interpolation method. To see to what extent damping is experienced in this model, we ran the basic model without the mean flow. With a time step of six minutes and a spatial separation of 20 km, the total loss in magnitude of the center vorticity value during the 72 hour period was $.33 \times 10^{-5} s^{-1}$, where the initial value was $217.46 \times 10^{-5} s^{-1}$. Due to this very slight amount of damping at our shortest time step, we believe the forecast track from the semi-Lagrangian forecast more truly reflects the correct forecast.

Throughout the 72 hours, while with both models the vortex center maintained its relative shape, the semi-Lagrangian model maintained the magnitude of the center slightly better by maintaining a tighter vorticity gradient at 72 hours as seen in Figure 3 on page 15. In this basic comparison, it is difficult to say which model was better. While the semi-Lagrangian model gave a slightly better forecast, the finite difference model was definitely more economical when considering computer resources. For an equal $M \times M$ grid, the size of the memory region needed to be increased by one third for the semi-Lagrangian model due to the calculation of the bicubic coefficients. Also the run time for the semi-Lagrangian model was three and one half times the time required for the finite difference model to run. The vortex track from the finite difference scheme also is improved when we follow the streamfunction minimum.

B. TIME STEP VARIATIONS

As stated in the introduction, one of the semi-Lagrangian model's significant features is its ability to give an accurate forecast while extending the time step. In the next experiment, we tested the model with varying time steps. Our comparison finite difference model, which is restricted by the CFL condition $U \frac{\Delta t}{\Delta x} < .707$, became unstable at a time step slightly less than seven minutes. Therefore we could not compare the semi-Lagrangian model with the finite difference model.

When we doubled the time step to twelve minutes we saw some improvement in the semi-Lagrangian models forecast through 48 hours. This was expected due to the fewer number of interpolation steps required. This basically agrees with the findings in Robert (1981) that there is no appreciable truncation error added as the time step is increased. The vorticity maximum showed less damping while the track remained smooth both in direction and speed. This also decreased the overall CPU time to almost one third of that required at a time step of six minutes. Continuing in this same vane, the same type of improvement was expected when tripling the time step to eighteen minutes. Though

at this point, we no longer had quick convergence of the iteration scheme for calculating the displacement values. Pudykiewicz & Staniforth (1984) referenced the fixed point theorem of Conte & Deboor which states that the convergence of the iterative technique is assured provided that the first partial derivatives are continuous, that Δt is sufficiently small, and that the first guess is sufficiently close to the true solution. The condition derived by Pudykiewicz & Staniforth in their paper for convergence is of the form

$$\Delta t \max(|u_x|, |u_y|, |v_x|, |v_y|) < 1 \quad (3.1)$$

The shear seen in a strong tropical system as depicted in this model given by the profile in chapter two is on the order of $4.0 \times 10^{-4} s^{-1}$. The maximum Δt for continued convergence is less than 41 minutes which is lower than those seen in other studies reviewed. The values of the displacements at six and twelve minutes show that at the shorter time step the displacement stayed within one grid region. At twelve minute time steps, the displacements in the region of the vortex came from two or three grid regions away along a curved trajectory. Thus, the first guess becomes increasingly less accurate as compared to the true solution for points near the vortex. As we increased the time step, the number of iterations increased from two iterations at six minutes, to six iterations at 12 minutes, to 30 at 18 minutes. Computing resources limited further testing of increasing the time step. It is seen as stated in Kuo and Williams (1989), that the semi-Lagrangian application is limited by the variation in velocity and in this study by the curvature of the flow. Table 2 on page 12 provides the relative magnitude of the vorticity maxima during the different integrations of the semi-Lagrangian model and the comparison finite difference forecast for the first 48 hours. The magnitude is taken as the maximum value at a grid point.

At this point, we looked at the results as we lowered the level of accuracy required in the iterative step. As stated in Chapter II, the error bound set for the semi-Lagrangian model was 1.0×10^{-5} . Little improvement was seen with higher levels of accuracy in displacement during our initial tests with a time step of six minutes. In the following experiment, a time step of 15 minutes was used. Three integrations of the semi-Lagrangian model were run. The first run had a error bound of 1.0×10^{-3} to control the number of iterations to find the displacements. Two iterations were required to meet this restriction set. As expected, the forecast was much less accurate with significant damping. The two other integrations of the model were completed with an error bound of 1.0×10^{-4} requiring three iterations to meet and 1.0×10^{-5} requiring ten

Table 2. MAGNITUDE OF VORTEX FOR DIFFERENT ITERATIONS OF MODEL

	FD 6 min	SL 6 min	SL 9 min	SL 12 min
0 hr	217.46	217.46	217.46	217.46
6 hr	173	183	186	189
12 hr	172	174	178	182
18 hr	171	171	176	176
24 hr	166	169	175	175
30 hr	167	166	173	172
36 hr	162	164	170	170
42 hr	156	163	168	170
48 hr	153	161	168	174

iterations, respectively. The 12, 24 and 36 hour forecasts for each of the three integrations are shown in Figure 4 on page 16. In run one with the largest error bound, the vortex streamfunction pattern is much weaker than the other two runs. The vorticity field also loses its symmetric shape during the first twelve hours with the lower number of required iterations. The second and third runs are comparable through the first 18 hours thereafter, run two with an error of 1.0×10^{-4} begins to show more damping and a distortion of the vorticity field. Run three produced a forecast as accurate as the forecast run at a time step of six minutes seen in Figure 3 on page 15. Table 3 on page 13 provides the relative magnitude of the damping effects at lower error restrictions. Values presented again are the maximum value at a grid point.

Wide differences in the center's position also occurred with runs one and two. Inconsistencies in the velocity and direction of the vorticity maximum's movement was experienced. When we returned to our "ideal" error of 1.0×10^{-5} , the track returned to the smooth forecast expected with the semi-Lagrangian method. Figure 5 on page 17 shows the forecast tracks from each of the three runs.

C. GRID SIZE VARIATIONS

Numerical modeling by finite difference models has also been limited by the spacing of the grid points. We know that the numerical solution will be more accurate when the grid size, Δx , is small or in other words, when there are many grid points to resolve a given wavelength than when there are few (Haltiner & Williams, 1980). With this in

Table 3. MAGNITUDE OF VORTEX WHEN VARYING DISPLACEMENT ACCURACY

	.001	.0001	.00001
0 hr	217.46	217.46	217.46
6 hr	156	180	189
12 hr	144	162	177
18 hr	134	149	170
24 hr	134	142	168
30 hr	129	131	166
36 hr	127	128	164
42 hr	121	124	162
48 hr	122	116	162

mind, we experimented with doubling the grid spacing in both the semi-Lagrangian model and the finite difference model. Again we used a time step of six minutes for the comparison. The tracks of both model forecasts are shown in Figure 6 on page 18. As with the lower resolution experiments, the finite difference track shows more oscillations from a smooth track. The observed inaccuracies noted can be attributed to the process in which the vortex is found when using a finite difference scheme. In a finite difference scheme, the vortex center is located within a grid space by bi-linear interpolation only. When the resolution is increased, the error caused by the bi-linear interpolation scheme is greatly reduced and the track becomes smooth with less oscillations in the speed of the vortex center. Also as stated previously as the streamfunction field in the finite difference model is smoother, following the streamfunction minima would give a smoother track. For the first 12 hours, both models maintained equal magnitudes of vorticity, but it took longer for the interpolation routine of the semi-Lagrangian method to settle out causing an increase in magnitude loss with the semi-Lagrangian forecast.

As stated in the introductory chapter, the semi-Lagrangian method gives smaller phase errors and is not effected by computational dispersion as finite difference models are. Spatial differencing in the finite difference schemes tends to cause an under estimate of the phase speed for the short waves. After Haltiner and Williams (1980), with a second order finite difference scheme, the speed of the numerical wave is always less or at

most equal to the true wave speed. In addition to as $\Delta x/L \mapsto 0$, where L equals the wavelength, the phase speed of the finite difference wave is equal to the true speed. Waves that are relatively long compared to Δx have little phase speed error.

Computational dispersion, a source of error in forecast models, occurs because the numerical phase speed varies with the wavelength where the true phase speed is constant for all wavelengths. Figure 7 on page 19 shows how the finite difference model became distorted as time passed. The shorter wavelengths are seen trailing the longer waves. The semi-Lagrangian model more closely resembles the true solution which has the same phase velocity for all wavelengths.

D. SUMMARY

In summary of this chapter's results, we saw that both models gave comparable forecasts at a time step of six minutes, though the semi-Lagrangian with its need for more calculations is not as efficient. As expected, the forecast ability of the semi-Lagrangian model improved as we lengthened the time step. Though, due to the shear and curvature experienced with the vortex, large time steps of over one hour were not practical. Further research into changing the accuracy on the displacements, found in this case with a strong cyclone restricting the model to a predetermined number of iterations or applying a mean error restriction across the grid is not optimal. An experiment done by setting an error bound of 1.0×10^{-3} on the displacement values of the inner 60 grid points required an average of six iterations to meet. A fairly accurate forecast was produced through 12 hours as seen in Figure 8 on page 20. A large difference can be seen between these results and those shown in Figure 4 on page 16 which was completed with a average error bound of 1.0×10^{-3} placed over the entire grid. In the future, it is suggested that a set error bound for the displacement be calculated at each grid point. In this code, the bicubic spline routine was not optimal for this use as it calculates over an entire field vice a single point.

The experiments with grid spacing proved that the semi-Lagrangian gives good phase speed and is not hampered by computational dispersion experienced with the finite difference models.

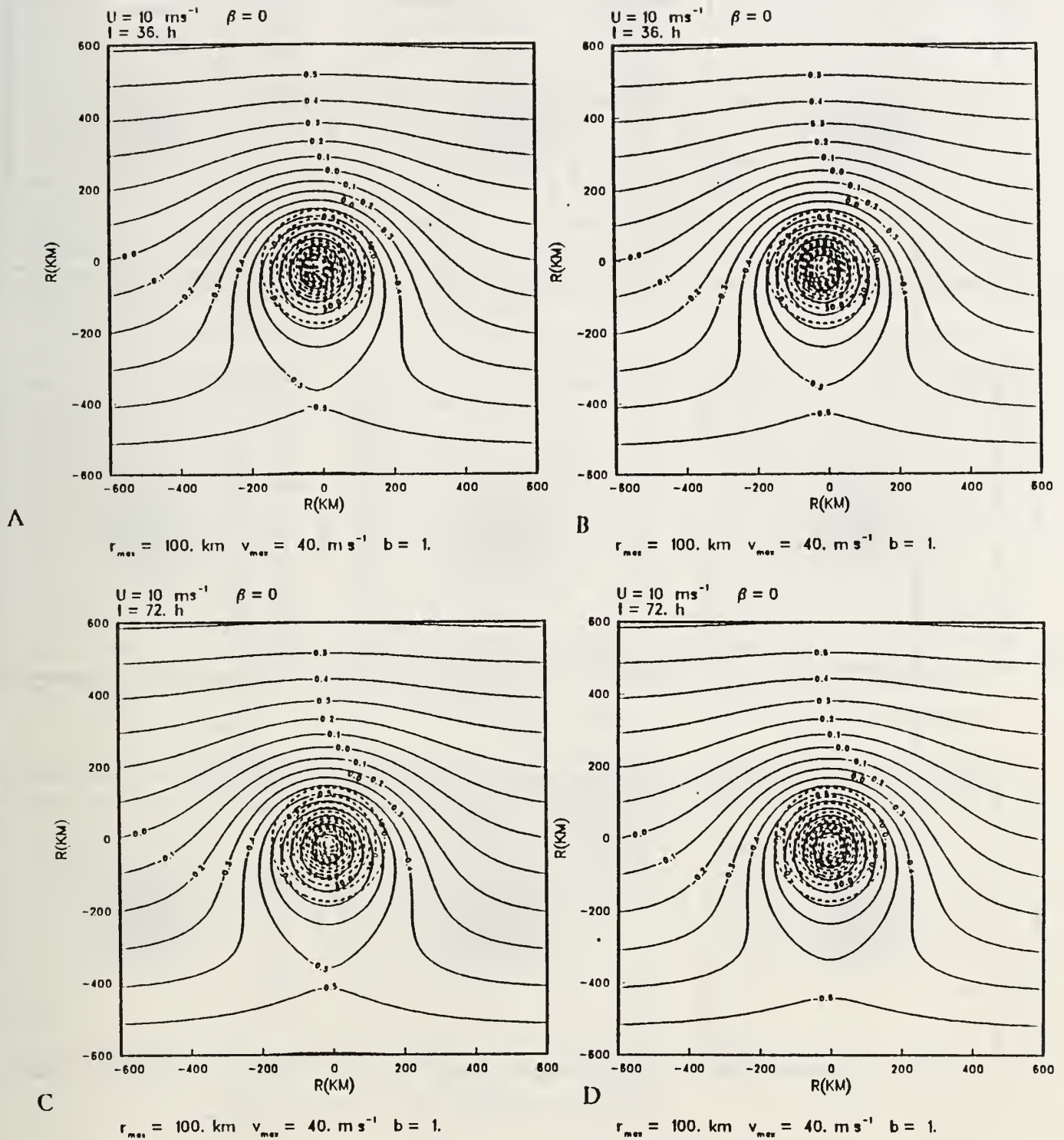


Figure 3. Basic Comparison Forecast: Finite Difference (FD) and Semi-Lagrangian (SL) Models. Streamfunction (solid), Vorticity (dashed), Time Step = 6 min, Grid Interval = 20 km. (a) FD Tau 36. (b) SL Tau 36. (c) FD Tau 72. (d) SL Tau 72.

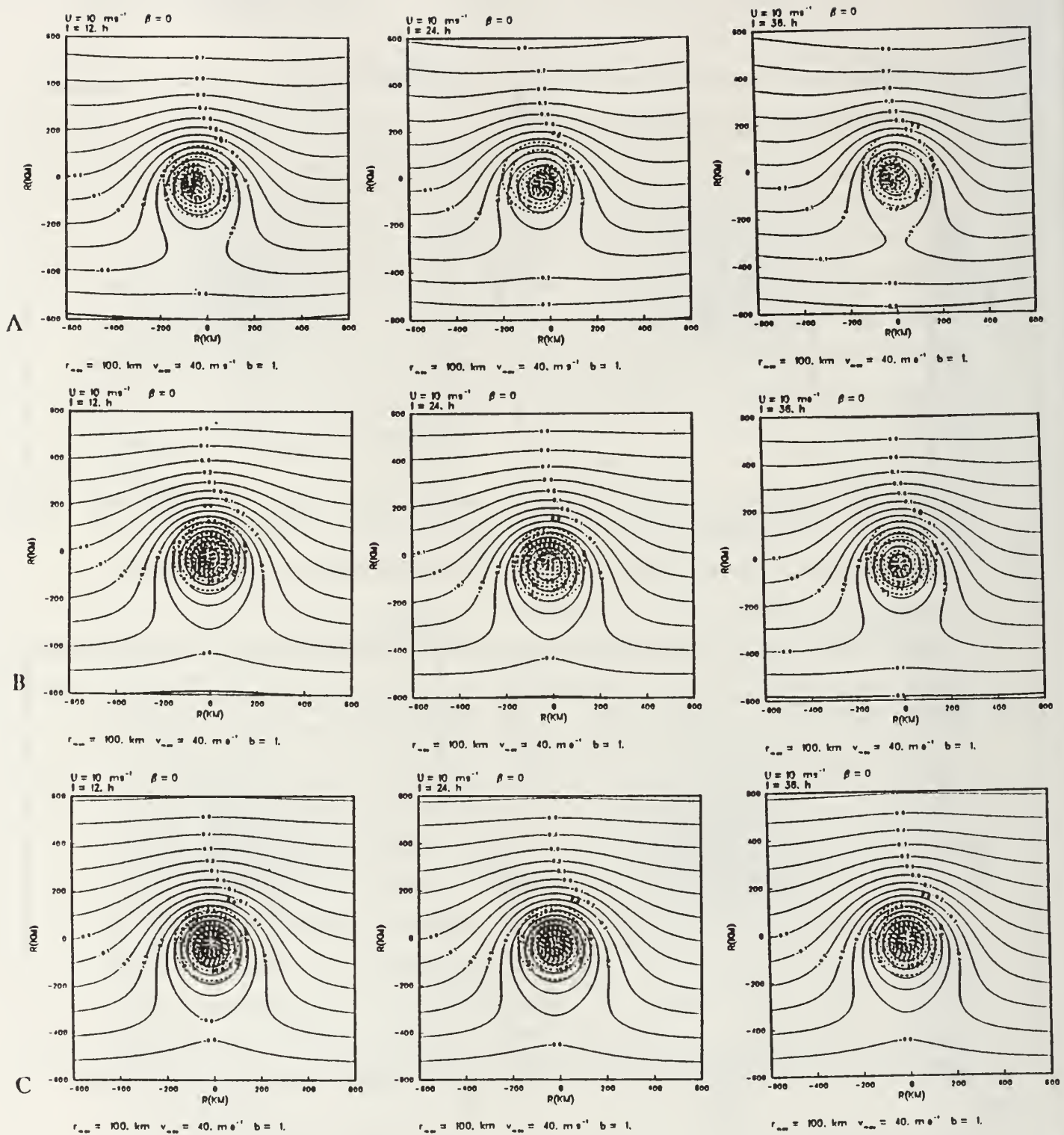


Figure 4. Varied Error Restrictions Forecast: Semi-Lagrangian Model, Streamfunction (solid), Vorticity (dashed), Time Step = 15 min, Grid Interval = 20 km. (a) .001 (b) .0001 (c) .00001.

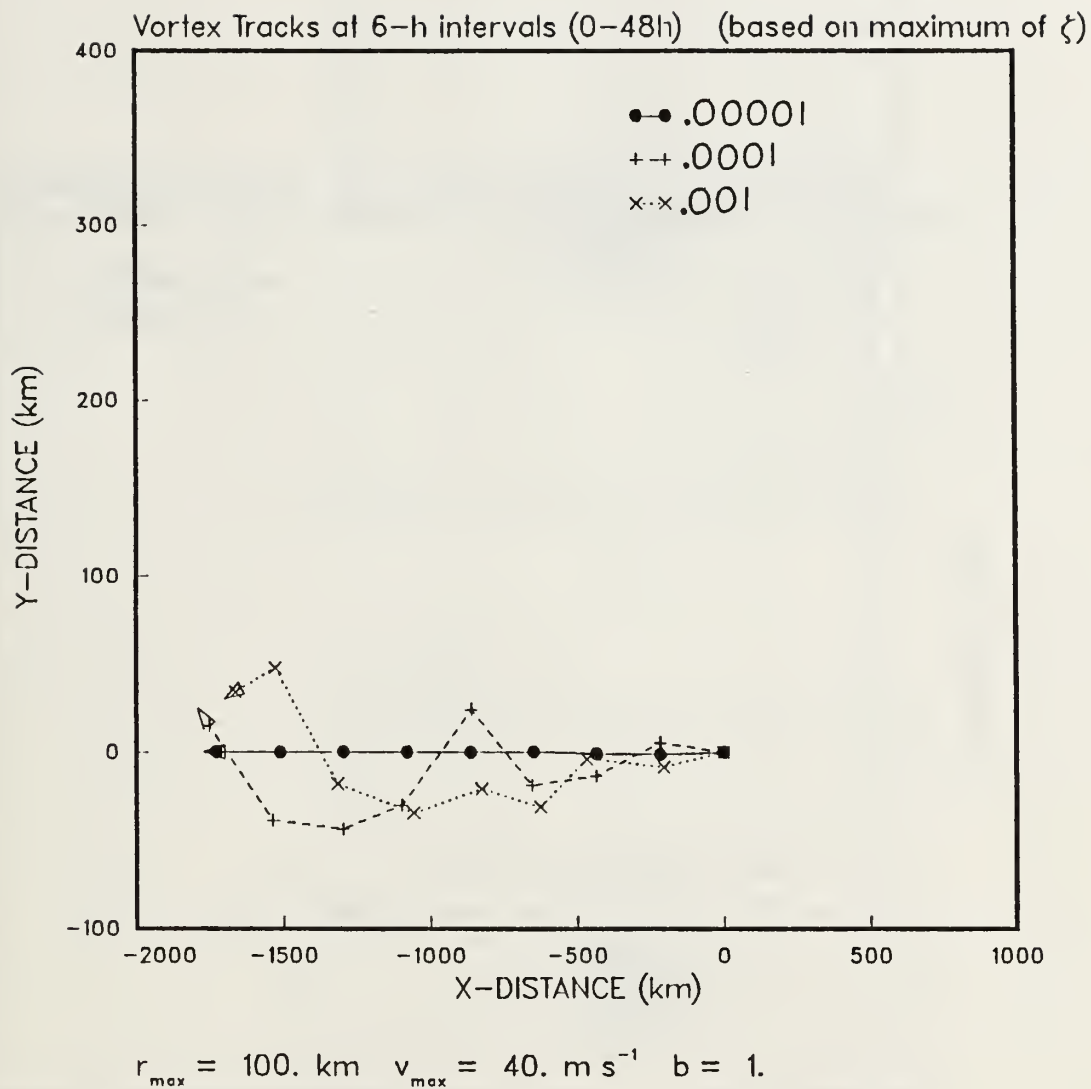
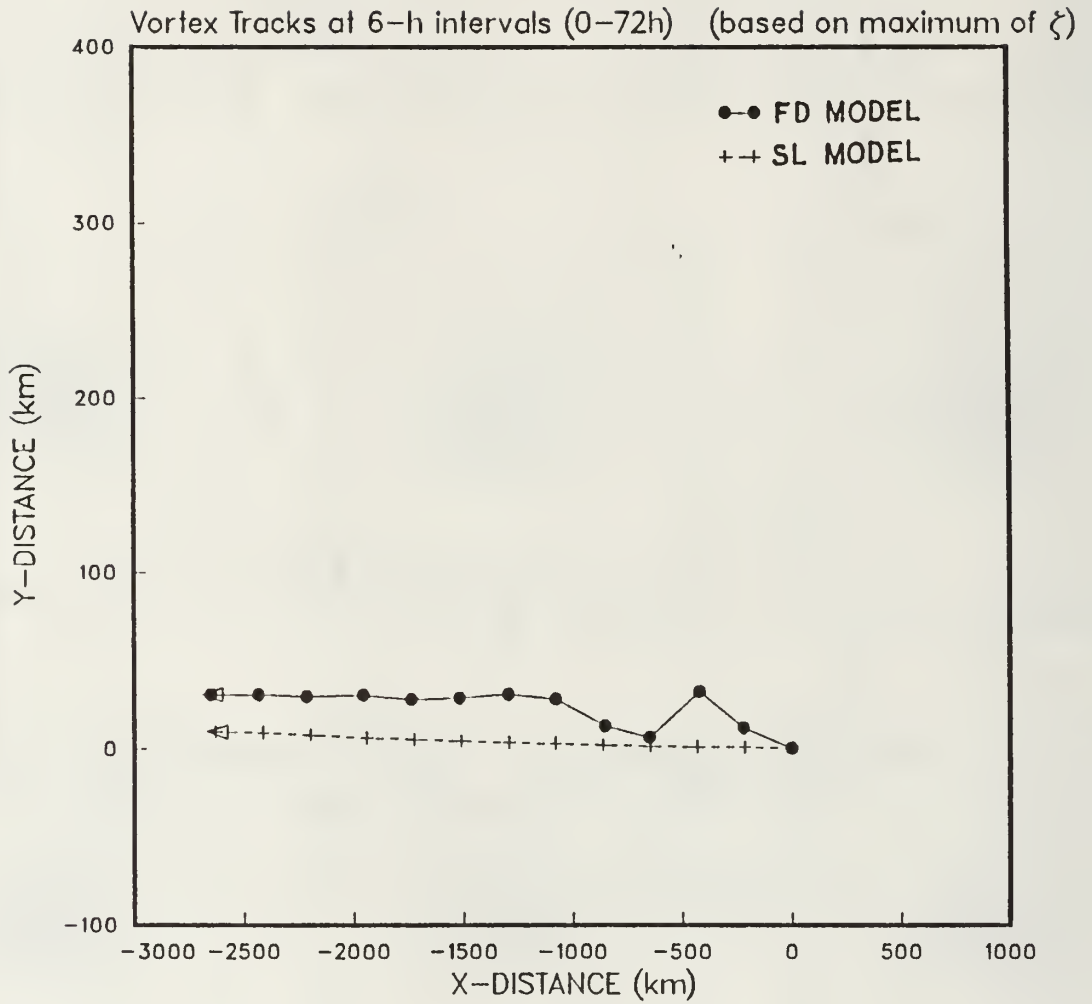
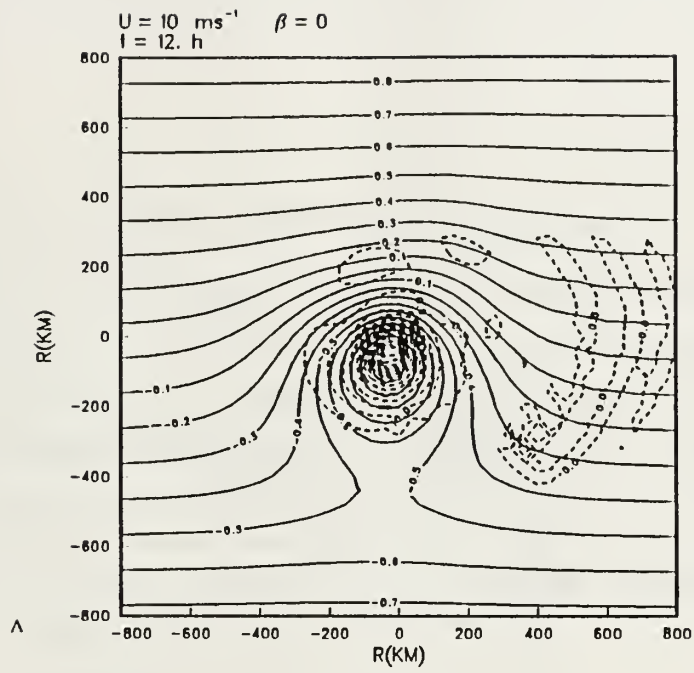


Figure 5. Varied Error Restriction Forecast Tracks: Semi-Lagrangian Model, Time Step = 15 min, Grid Interval 20 KM.

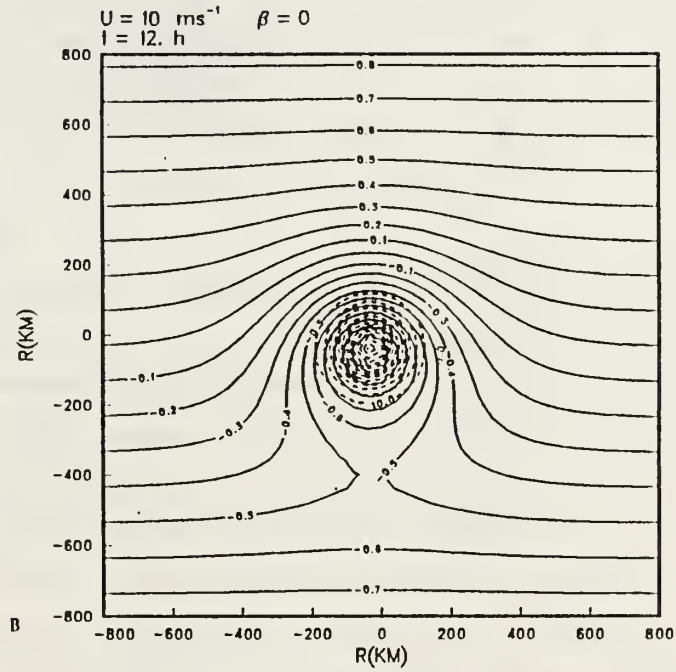


$$r_{\max} = 100. \text{ km} \quad v_{\max} = 40. \text{ m s}^{-1} \quad b = 1.$$

Figure 6. Grid Size Variation Comparison Forecast Tracks: Finite Difference and Semi-Lagrangian Models, Both models run with a Time Step of 6 min and a Grid Interval of 40 KM



$$r_{\max} = 100. \text{ km} \quad v_{\max} = 40. \text{ m s}^{-1} \quad b = 1.$$



$$r_{\max} = 100. \text{ km} \quad v_{\max} = 40. \text{ m s}^{-1} \quad b = 1.$$

Figure 7. Grid Size Variation Comparison Forecast: Finite Difference (FD) and Semi-Lagrangian (SL) Models, Streamfunction (solid), Vorticity (dashed). Both models run with a Time Step of 6 min and a Grid Interval of 40 km. (a) FD Tau 12. (b) SL Tau 12

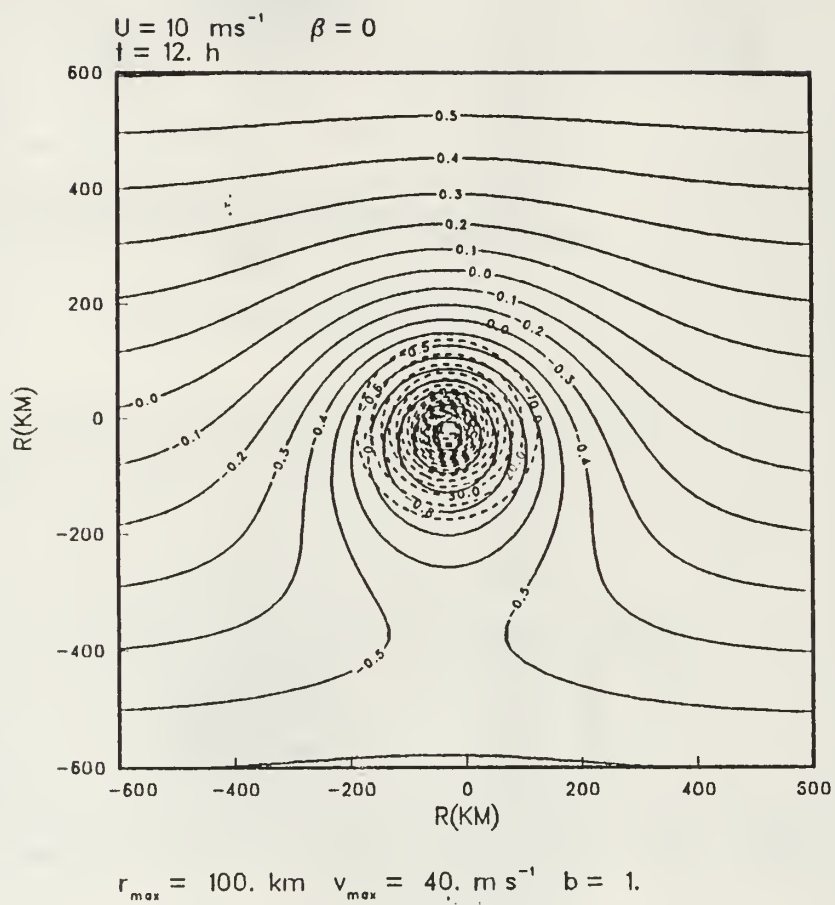


Figure 8. Error Restriction Test: Semi-Lagrangian model with error restriction set to .001 for inner points. Streamfunction (solid), Vorticity (dashed). Tau 12

IV. BETA DRIFT AND MODEL ACCURACY

It has long been known that tropical cyclones have a tendency to move poleward and westward even in the absence of any mean flow. This is the essence of the Beta Drift Theory. In Chan and Williams (1987), it was proven both analytically and numerically using a nonlinear model that the Beta term has two major effects. One, is the elongation westward of the vortex and the asymmetrical distribution of the winds. Second, is the northwest advection of the vortex. In this chapter, we will compare the results of our semi-Lagrangian model to the finite difference model used by Chan and Williams (1987) and Peng and Williams (1989).

A. NO MEAN FLOW EXPERIMENTS

In these experiments, the mean flow was excluded. In the first experiment, we performed a basic comparison between the semi-Lagrangian and the finite difference model using the same time step and spatial resolution. In the next few experiments, we increased the time step as in Chapter III keeping the grid size the same. Lastly, we varied the grid size to see what effect it would have on the forecast.

1. Basic Comparison

In the basic comparison, we looked at the semi-Lagrangian model and the finite difference model results run with our control values of a time step of six minutes and the grid size of 20 km. The stream function and vorticity fields for the semi-Lagrangian model at 0, 24, 48 and 72 hours are given in Figure 9 on page 27. Similar to the run made by the finite difference model, the vortex is seen to elongate westward. Chan and Williams in their 1987 paper explained the westward elongation to be a result of the dispersive effects of the rossby waves or also termed the "linear beta effect". The slight southwest-northeast tilt has been explained by previous research to be due to the interaction of the linear beta effect and the nonlinear advective terms. As with the earlier study with the finite difference model, the wind pattern showed the development of a speed maximum to the northeast of the center and a minimum in the flow to the southwest. This asymmetry increases as the maximum wind increases as we progress through the forecast period. In this case without any mean flow advection, the finite difference model maintained significantly higher values of vorticity than the semi-Lagrangian model.

The tracks of the two model runs are shown in Figure 10 on page 28. The solid line is the semi-Lagrangian forecast which shows as in the basic comparison of Chapter III that it maintained a smoother forecast track than that of the finite difference model. As seen in Chan and Williams (1987), our model also shows an increasing speed of advance of the vortex from .6 m/s during the initial six hour forecast period to 2.9 m/s during the last six hours of the forecast. Further investigation into the speed of the vortex movement showed a period of rapid growth in the translation speed between six and 12 hours, near linear growth between 12 and 48 hours and a steady growth period after 48 hours which follows results found in Fiorino and Elsberry (1989). The north-west displacement and the acceleration of the vortex center are similar to those seen by Chan and Williams and attributed to the development of the east-west asymmetry induced by the Beta effect. Table 4 on page 23 gives the six hourly direction and speed for each of the two runs. In their study, Chan and Williams saw significant oscillations in the forecast track, though with the semi-Lagrangian forecast the direction was more constant, varying within three degrees of 329 degrees. The finite difference scheme varied between 317 and 350 degrees. The consistency of the semi-Lagrangian scheme here is related to the smoothness of the vorticity field while with the finite difference scheme the vorticity field is much noisier. In the finite difference model if we would track the streamfunction minimum, the forecast tracks would be more similar. The speed of movement in the semi-Lagrangian forecast was also more constant leveling off or decreasing slightly at the end of 72 hours.

2. Time Step Variations

Again as in Chapter III, we ran the semi-Lagrangian model increasing the time step to nine minutes and then doubling it to twelve minutes. As before, we saw the number of iterations to achieve the acceptable error level increased as the time step increased. As seen before in the results in Chapter III, we had some improvement in the forecast in each run as we increased the time step. The magnitude of the vorticity increased slightly, 1% higher, at each forecast interval using a twelve minute time step then when using a six minute time step. The overall pattern of the streamfunction and vorticity fields at the time steps of six, nine and twelve minutes remained the same except for the earlier appearance of the weak anticyclonic circulation to the east of the vortex and the further elongation to the west of the outer streamfunction field as the time step increased. Figure 11 on page 29 shows the streamfunction and vorticity fields for (a) integration with the time step of nine minutes and, (b) a time step of twelve minutes.

Table 4. TRACK COMPARISON SEMI-LAGRANGIAN/FINITE DIFFERENCE

Hours	Semi-Lagrangian		Finite Difference	
	Dir	Spd	Dir	Spd
0-6	330.1 deg	.6 m/s	344.4 deg	.4 m/s
6-12	326.4 deg	1.2 m/s	322.3 deg	1.3 m/s
12-18	326.6 deg	1.6 m/s	330.8 deg	1.8 m/s
18-24	328.5 deg	2.0 m/s	328.5 deg	1.9 m/s
24-30	327.7 deg	2.3 m/s	326.0 deg	2.2 m/s
30-36	328.1 deg	2.5 m/s	332.6 deg	2.9 m/s
36-42	329.5 deg	2.7 m/s	316.8 deg	2.7 m/s
42-48	329.5 deg	2.8 m/s	350.3 deg	2.1 m/s
48-54	329.6 deg	2.9 m/s	327.0 deg	3.7 m/s
54-60	331.4 deg	2.9 m/s	325.6 deg	2.7 m/s
60-66	330.9 deg	2.9 m/s	337.9 deg	2.8 m/s
66-72	332.2 deg	2.9 m/s	328.4 deg	3.0 m/s

increased. Figure 11 on page 29 shows the streamfunction and vorticity fields for (a) integration with the time step of nine minutes and, (b) a time step of twelve minutes. In turn, the component wind fields maintained speeds also up to 1% higher as we increased the time step from six to 12 minutes.

Figure 12 on page 30 shows the forecast track for both the six minute and twelve minute run through 72 hours. As one can see, with the increase in time step, the vortex position reached points further to the northwest. Again when looking at the translation speeds between subsequent positions, we were able to see the same general pattern as we saw using a six minute time step.

The question arose as to why do we saw this advance in position with increased time steps. Fiorino and Elsberry (1989) discussed that subtle changes in the outer vortex structure may lead to significant track deviations. They indicated that changes on the order of 1-3 m/s in the wind field have a significant effect on the track. An experiment to see what changes in the symmetric vortex's mean wind profile occurred during each of the runs was performed. It showed that at a radii of 100 to 500 km the mean wind field was maintained slightly stronger at a time step of 12 minutes compared to that at

3. Grid Size Variations

A difficulty often encountered in the tropical regions is the inadequate amount of observed data for model initialization especially when dealing with fine mesh grids. As seen earlier in Chapter III, the semi-Lagrangian model performed well when we used a coarser grid. No spurious errors were added to the forecasts. Figure 13 on page 31 is the streamfunction and vorticity fields for $\tau = 0, 24, 48$ and 72 with the grid spacing interval increased from 20 km to 40 km. The time step is 12 minutes. In comparison to Figure 9 on page 27 a forecast run at a 20 km resolution and a 12 minute time step, the streamfunction pattern is very similar. The noticeable difference is in the vorticity pattern. As noted in Chapter III, there is a large loss in the magnitude of vorticity between the initial and the 18 hour forecast as we increased the grid spacing. The magnitude of the center vorticity at the 72 hour forecast with a spatial interval of 40 km is $117 \times 10^{-5} s^{-1}$ while the center vorticity with a 20 km grid interval is at $165 \times 10^{-5} s^{-1}$. The damping associated with the interpolation scheme is more apparent with a larger grid interval.

The forecast track for this model integration is shown in Figure 14 on page 32. Again, the same growth pattern is seen in the translation speeds as is seen in the semi-Lagrangian forecast run at 20 km. Comparing the overall movement of the vortex between this run of the semi-Lagrangian model and the run at a time step of 12 minutes and a grid interval of 20 km, shows that the forecasts are nearly the same. A comparison to the finite difference forecast at a grid interval of 40 kilometers is also presented. As in Chapter III, the finite difference model's forecast track took greater departures from a straight line track at larger grid intervals.

In an effort again to see if the damping factor is responsible for the smoothness of the track, we ran another integration of the semi-Lagrangian model. In this integration, we used a grid interval of 10 km and a time step of six minutes. We compared the results to the run completed at a time step of six minutes and a grid interval of 20 km. The forecast track for the 10 km run is pictured in Figure 15 on page 33. Knowing that the interpolation scheme produces less damping with a smaller grid interval, we supposed that the small scale features that may have been masked by the damping at larger grid intervals would bring in track deviations. In this integration at 10 km, the vorticity magnitude was maintained at significantly higher values and the forecast track took less deviations in direction than the track with a greater grid interval. We also observed, that with the greater resolution run, the direction of motion of the vortex took on a more westerly direction though the overall distance travelled was similar.

observed, that with the greater resolution run, the direction of motion of the vortex took on a more westerly direction though the overall distance travelled was similar.

B. ASYMMETRIC CIRCULATIONS

Earlier studies have shown that the asymmetric circulation patterns are closely related to track orientation. In the following experiments, we look at the wave number one asymmetry in the azimuthal direction for our numerical model. This was obtained by Fourier analysis of the solutions patterned after work of Fiorino and Elsberry (1989). Figure 16 on page 34 shows the evolution of the wave number one gyre with time. This evolution compared closely to the results of Peng and Williams (1989). As in Fiorino and Elsberry (1989) which referred to these gyres as "Beta Gyres" the general features of the asymmetric streamfunction are the same for the semi-Lagrangian model. As they listed the pattern includes:

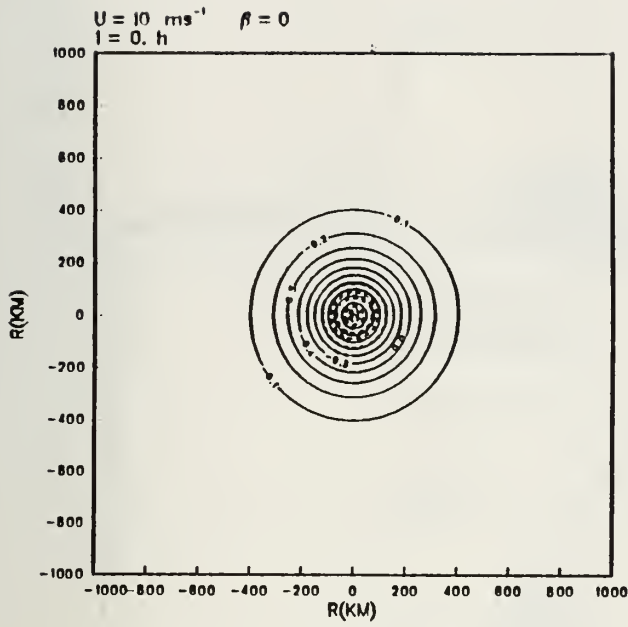
1. A dipole like pattern with an anticyclonic gyre on the east and a cyclonic gyre to the west of the center.
2. Straight flow between the centers of the cyclonic and anticyclonic gyres oriented to the northwest.
3. A small perturbation in the center of the pattern.

Figure 17 on page 35 shows how the amplitude of the streamfunction gyre increases with time. This figure is based on data from the model run at a time step of six minutes and a grid spacing of 20 km. The values are nondimensional. In their research, Fiorino and Elsberry showed that there were three phases to the growth pattern in the amplitude of the gyres. These were the rapid phase, linear phase and steady phase. The same basic pattern is seen here in our research and it correlates to the translation speed evolution.

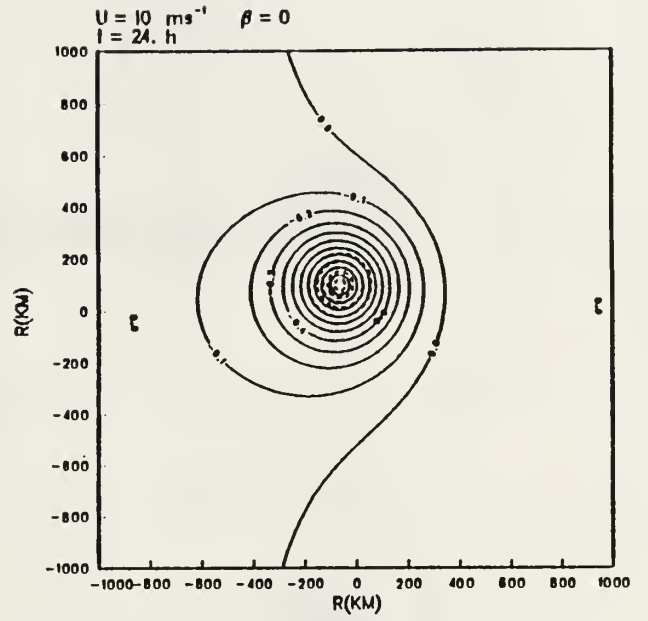
Figure 18 on page 36 shows how the growth in the amplitude changed between the six minute and the 12 minute run of the semi-Lagrangian model. As depicted, the overall pattern of growth did not change. The amplitude magnitude though was greater for the 12 minute run at all forecast intervals. The amplitude of the nine minute run fell between the six and 12 minute data. Note that at the end of the 72 hour forecast period we showed a slight decrease in the amplitude of the gyres and a slight slowing of the vortex translation speed. This data reinforces the interpretation made by Fiorino and Elsberry (1989) that there is a strong relationship between the vortex movement and the asymmetric circulation in the vicinity of the vortex's center.

C. SUMMARY

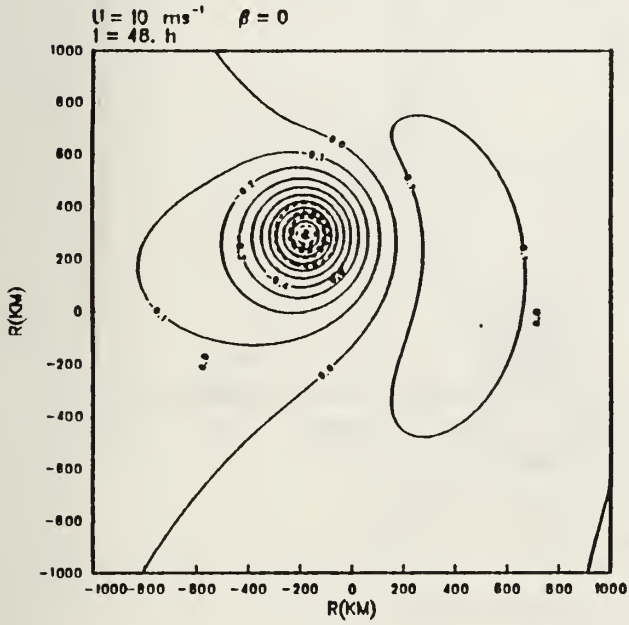
In this chapter, we ran experiments with and without the mean flow included. In each experiment, the forecast field changes in a way that had an effect on the movement of the vortex. Specifically, we saw changes in the outer wind fields which has been discussed in other research to be a possible cause in controlling vortex movement. Other experiments which were run revalidated that there exists a correlation between the evolution of the wave number one asymmetry and the change in the vortex's translation speed. The strength of the asymmetrical gyre and orientation of the "ventilation flow" were also seen to change as we varied the time step or the grid interval.



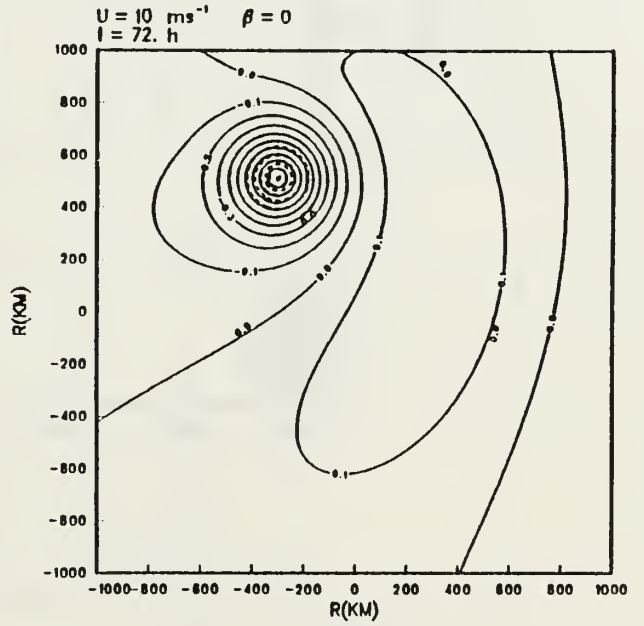
A $r_{\text{max}} = 100. \text{ km}$ $v_{\text{max}} = 40. \text{ m s}^{-1}$ $b = 1.$



B $r_{\text{max}} = 100. \text{ km}$ $v_{\text{max}} = 40. \text{ m s}^{-1}$ $b = 1.$



C $r_{\text{max}} = 100. \text{ km}$ $v_{\text{max}} = 40. \text{ m s}^{-1}$ $b = 1.$



D $r_{\text{max}} = 100. \text{ km}$ $v_{\text{max}} = 40. \text{ m s}^{-1}$ $b = 1.$

Figure 9. Semi-Lagrangian Forecast on a Beta Plane: Streamfunction (solid), Vorticity (dashed), Time Step = 6 min, Grid Interval = 20 km. (a) Tau 0, (b) Tau 24, (c) Tau 48, (d) Tau 72

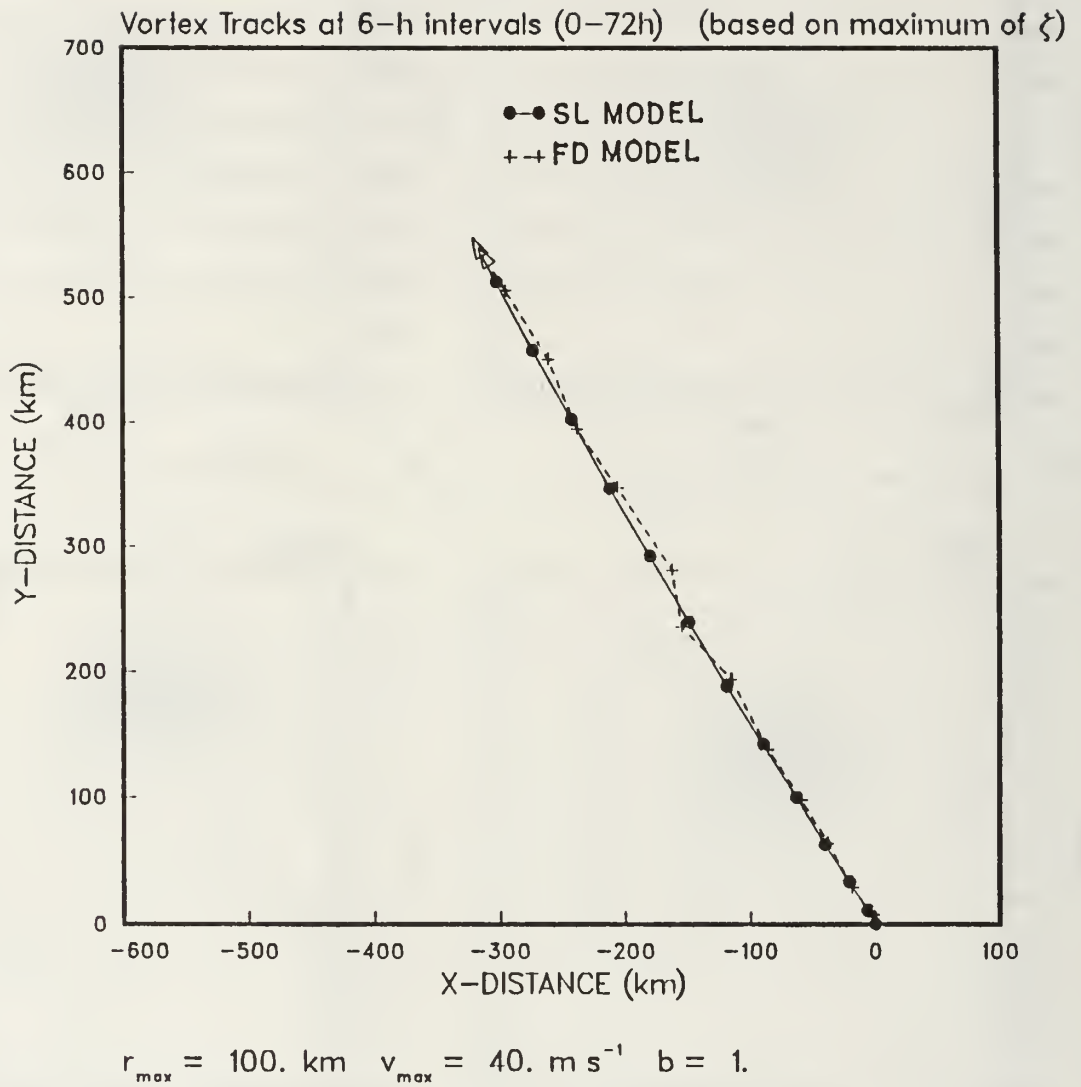


Figure 10. Basic Comparison Forecast Tracks with Beta: Semi-Lagrangian and Finite Difference Models. Both models run with a Time Step of 6 min and a Grid Interval of 20 km

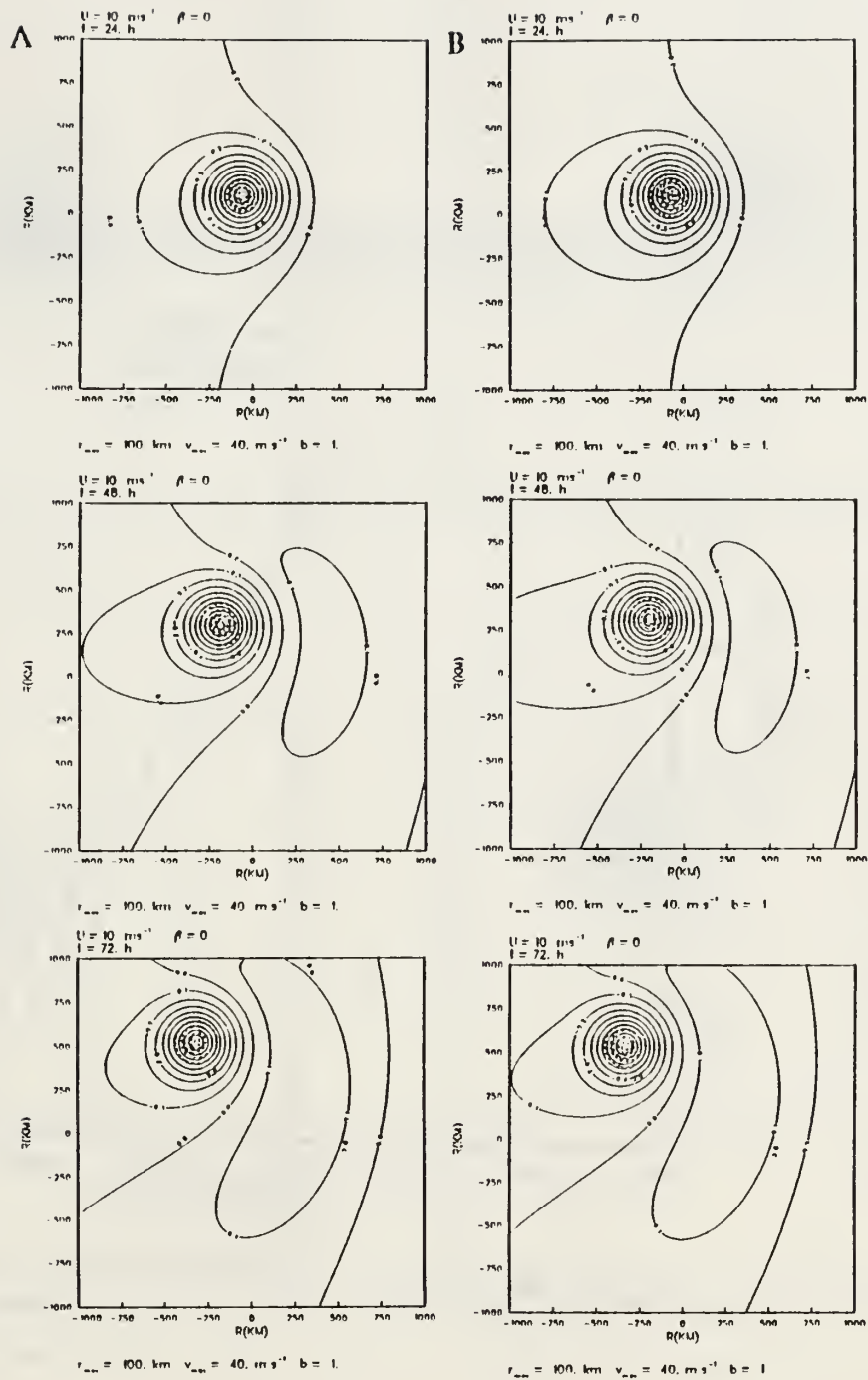


Figure 11. Semi-Lagrangian Forecast on a Beta Plane: Streamfunction (solid), Vorticity (dashed), Grid Interval = 20 km. (a) Time Step = 9 min, (b) Time Step = 12 min

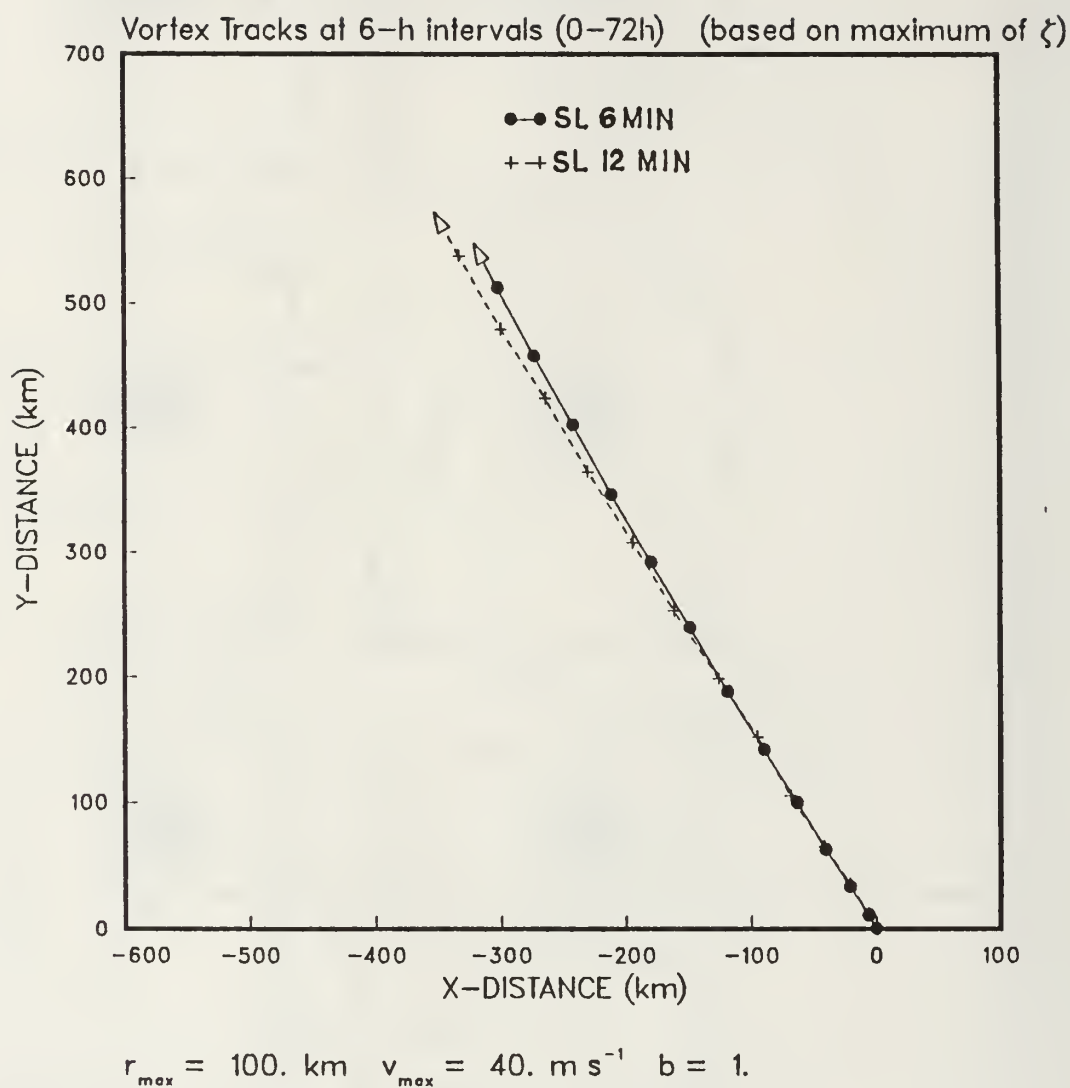
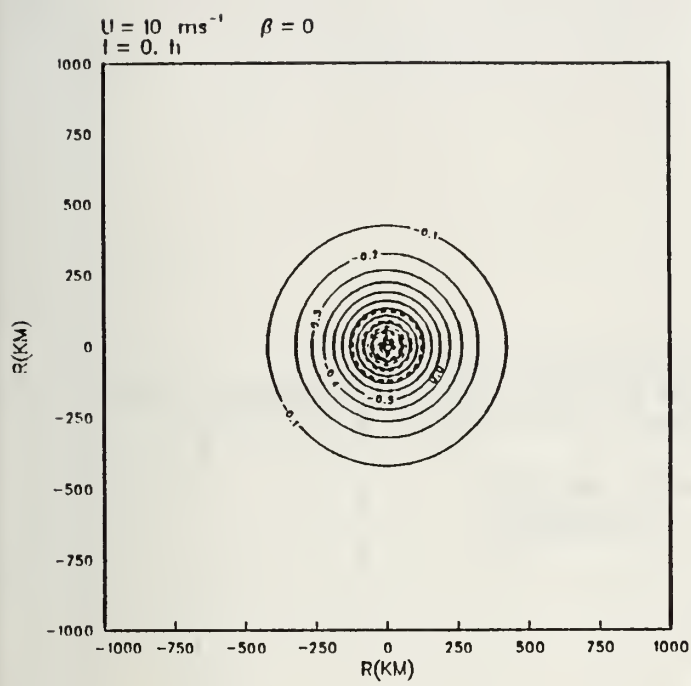
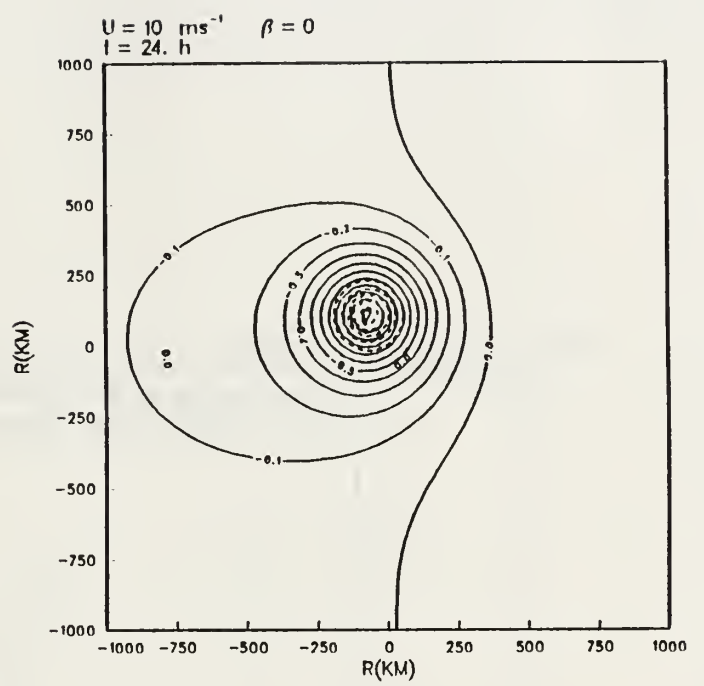


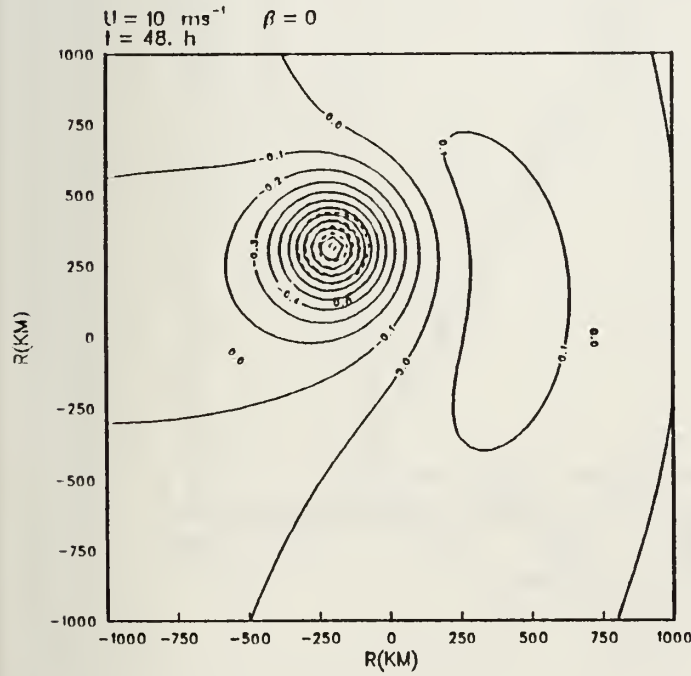
Figure 12. Semi-Lagrangian Forecast Tracks with Beta: Grid Interval = 20 km, Time Step = 6 min (solid), Time Step = 12 min (dashed)



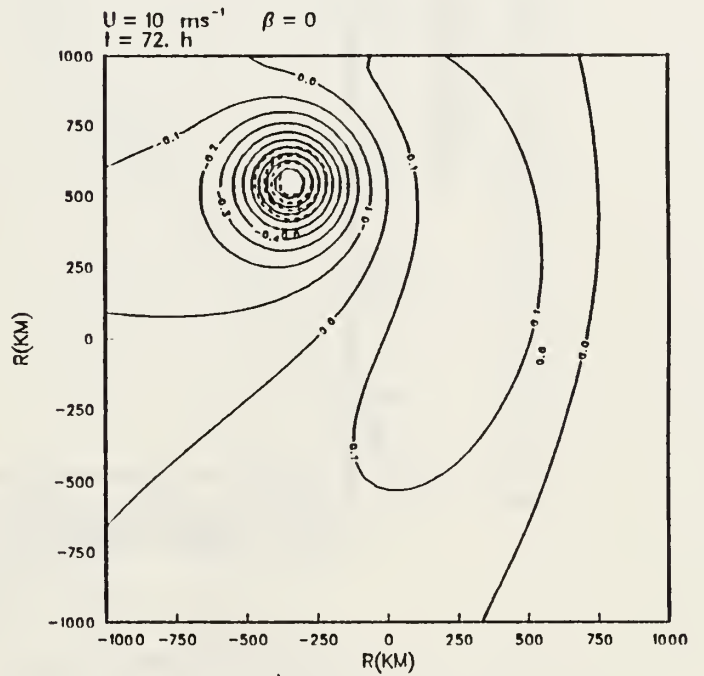
$r_{\text{max}} = 100. \text{ km}$ $v_{\text{max}} = 40. \text{ m s}^{-1}$ $b = 1.$



$r_{\text{max}} = 100. \text{ km}$ $v_{\text{max}} = 40. \text{ m s}^{-1}$ $b = 1.$



$r_{\text{max}} = 100. \text{ km}$ $v_{\text{max}} = 40. \text{ m s}^{-1}$ $b = 1.$



$r_{\text{max}} = 100. \text{ km}$ $v_{\text{max}} = 40. \text{ m s}^{-1}$ $b = 1.$

Figure 13. Grid Size Variation Forecast with Beta: Semi-Lagrangian model, Streamfunction (solid), Vorticity (dashed), Time Step = 12 min, Grid Interval = 40 km

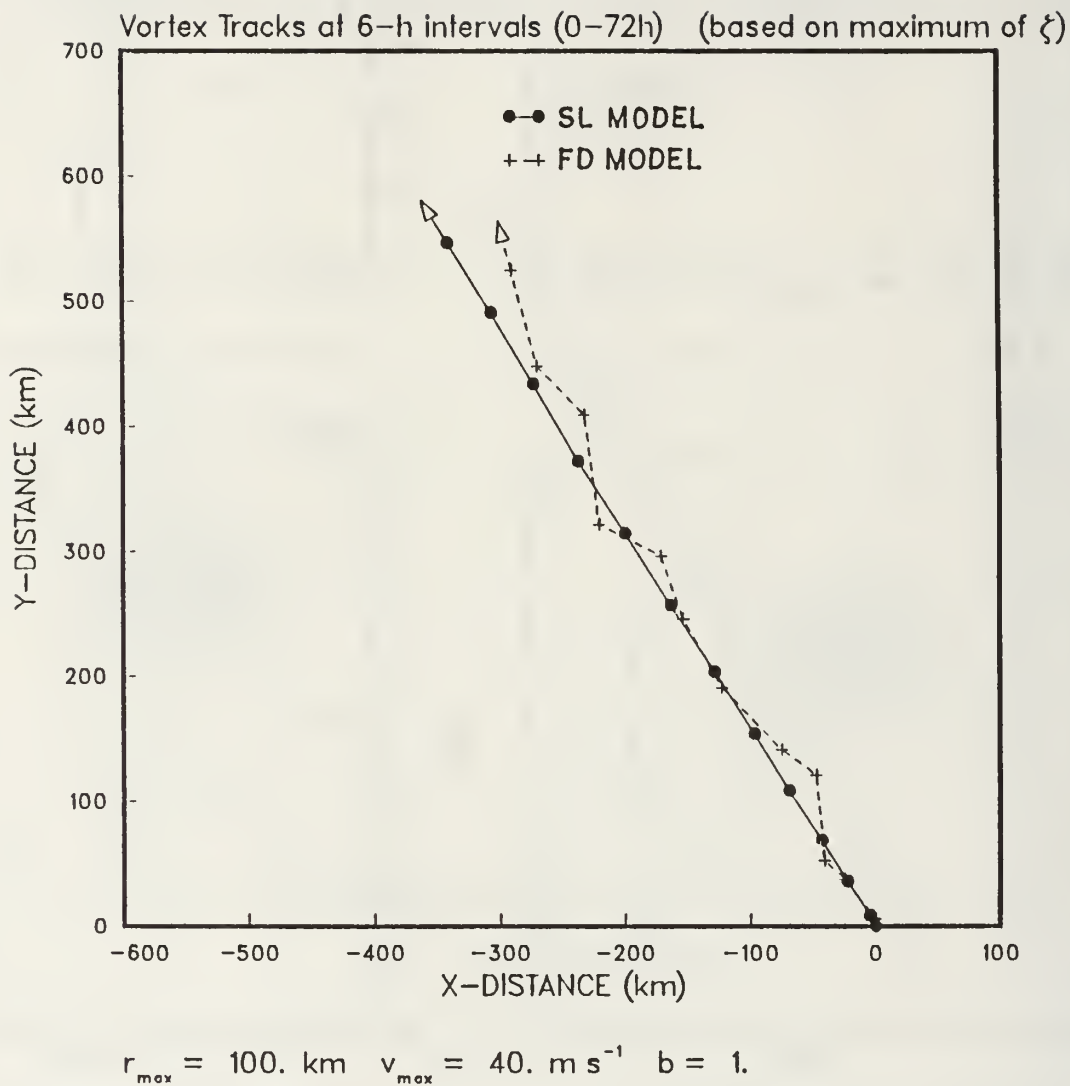


Figure 14. Grid Size Variation Forecast Tracks with Beta: Semi-Lagrangian and Finite Difference Models. Both models run with a Time Step of 12 min and a Grid Interval of 40 km

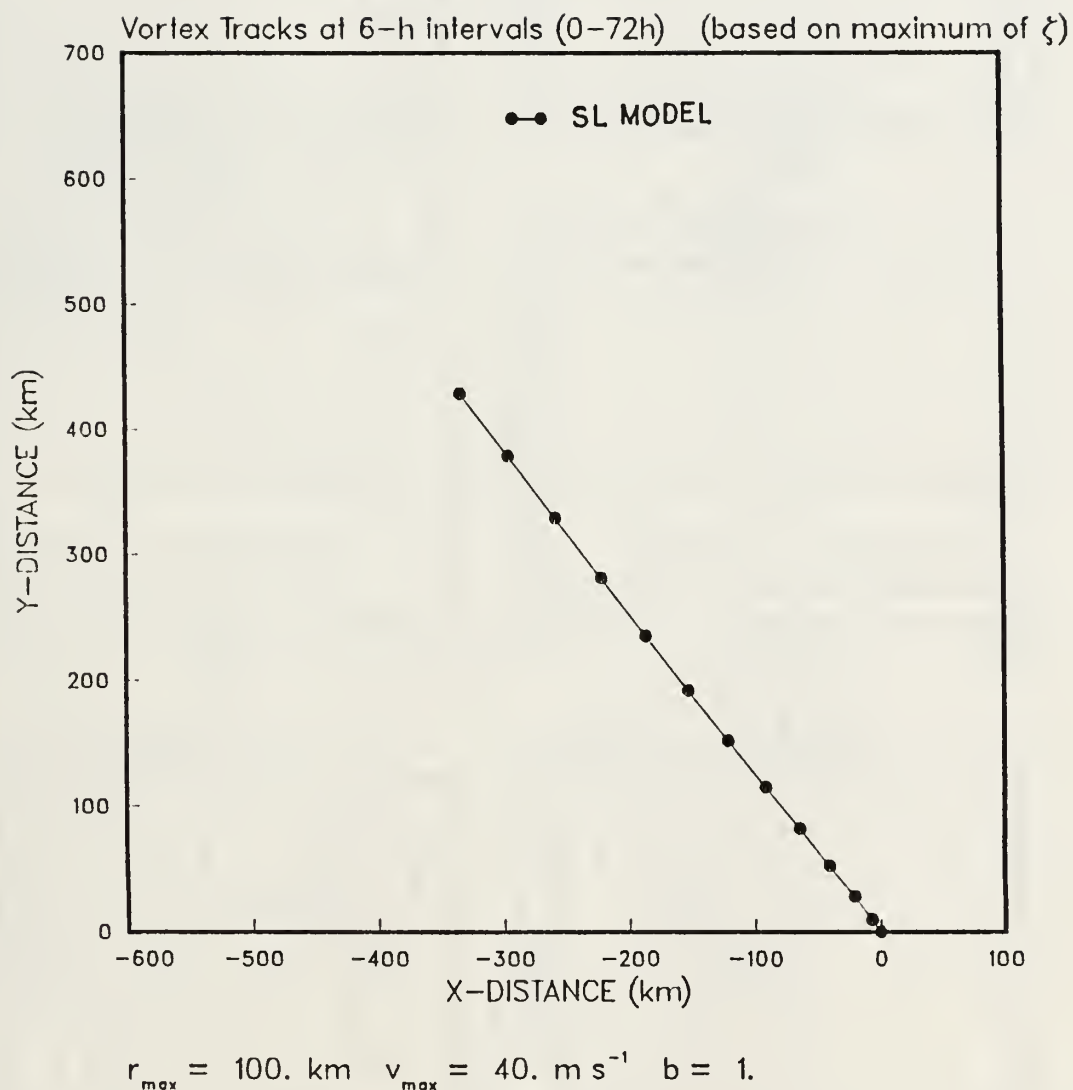
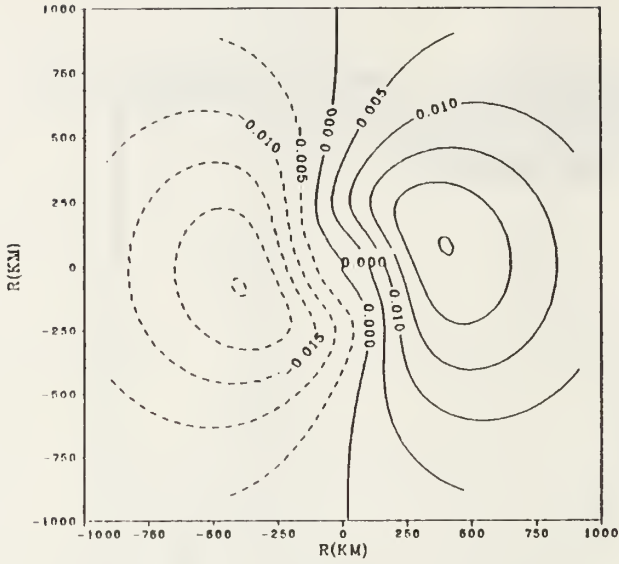


Figure 15. Grid Size Variation Forecast Track with Beta: Semi-Lagrangian Model, Time Step = 6 min, Grid Interval = 10 km

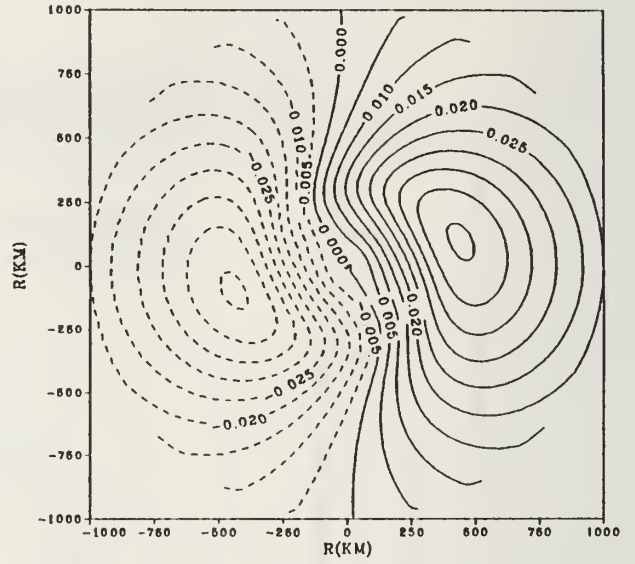
STR FN, CENTER=101.0, $\beta \neq 0$, NONLINEAR,

BEX = 1.0, VMAX = 40.0, TIME = 6.0, WAVE NO=1.1



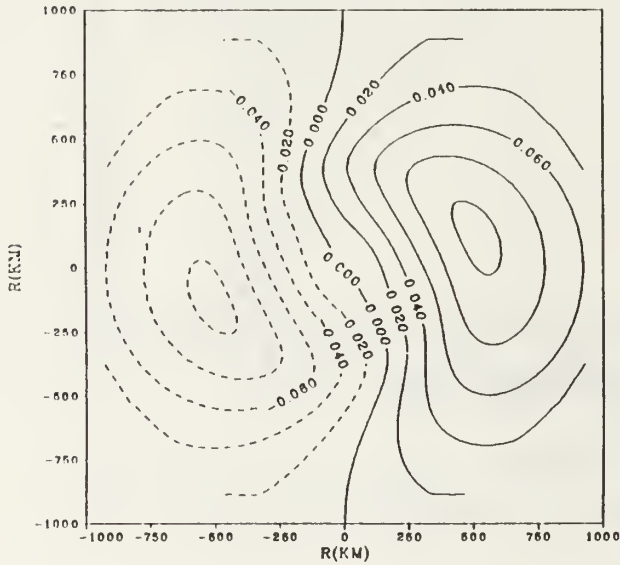
STR FN, CENTER=103.0, $\beta \neq 0$, NONLINEAR,

BEX = 1.0, VMAX = 40.0, TIME = 12.0, WAVE NO=1.1



STR FN, CENTER=110.0, $\beta \neq 0$, NONLINEAR,

BEX = 1.0, VMAX = 40.0, TIME = 36.0, WAVE NO=1.1



STR FN, CENTER=125.0, $\beta \neq 0$, NONLINEAR,

BEX = 1.0, VMAX = 40.0, TIME = 72.0, WAVE NO=1.1

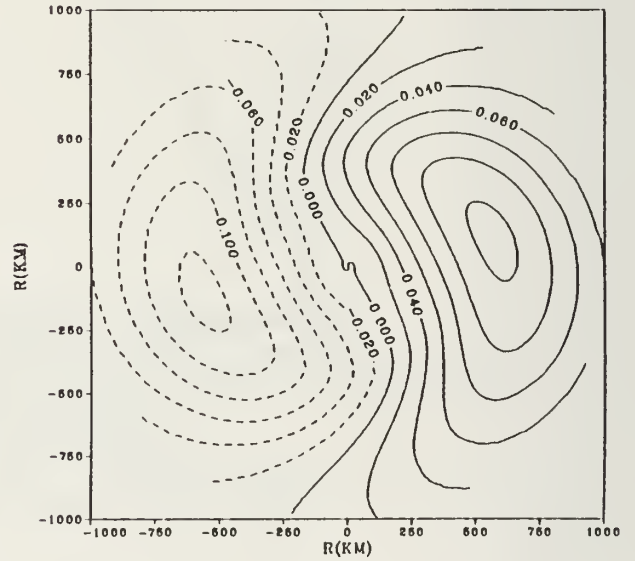


Figure 16. Wave Number One Gyre: Semi-Lagrangian Model, Time Step = 6 min, Grid Interval = 20 km

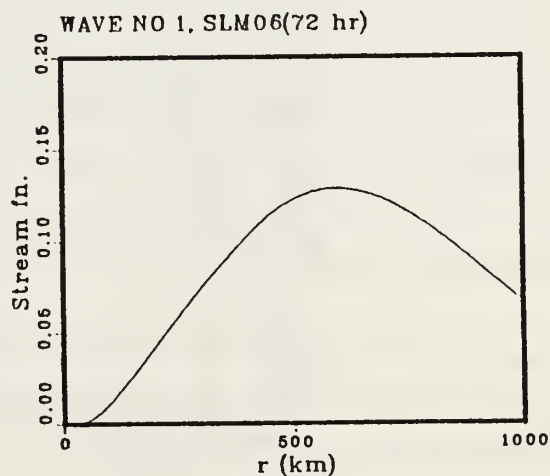
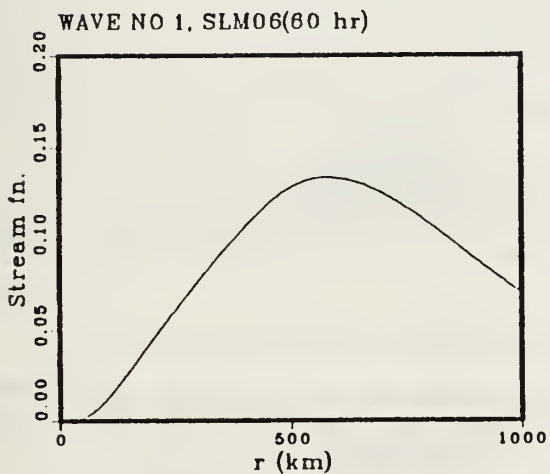
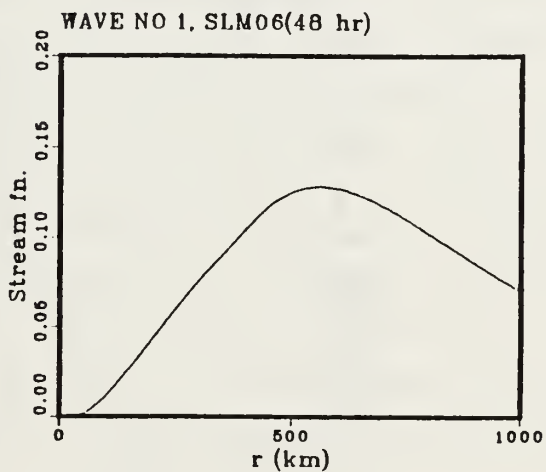
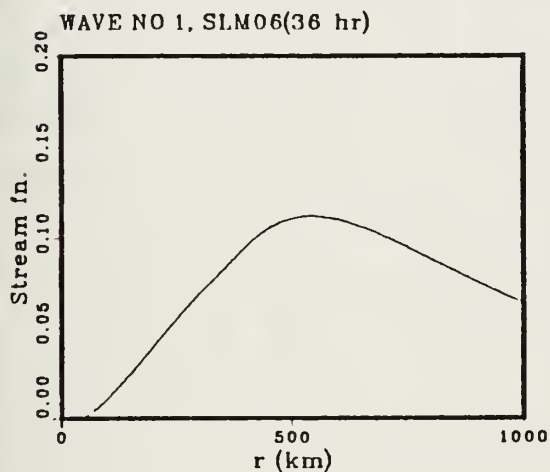
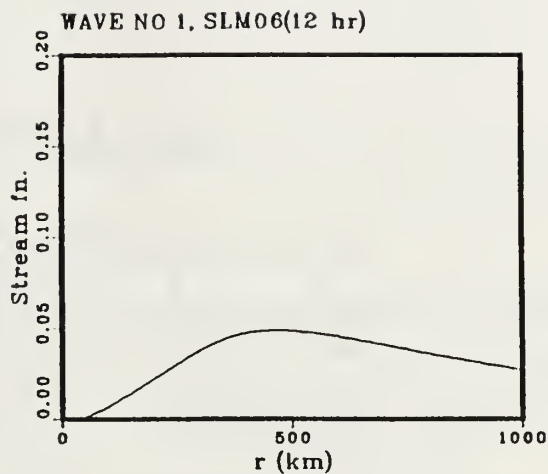
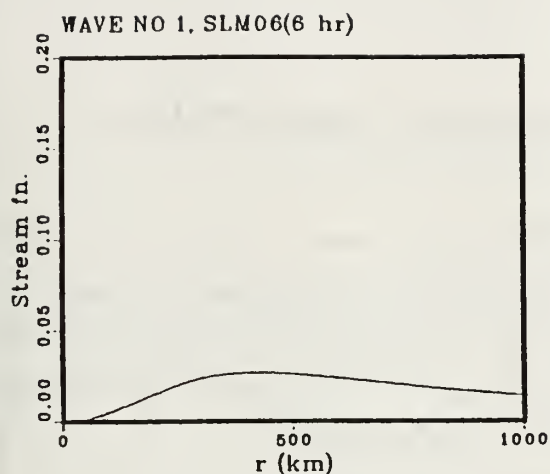


Figure 17. Wave Number One Amplitude Growth: Semi-Lagrangian Model, Time Series of Growth Tau 0 to Tau 72, Time Step = 6 min, Grid Interval = 20 km

STREAMFUNCTION AMPLITUDE

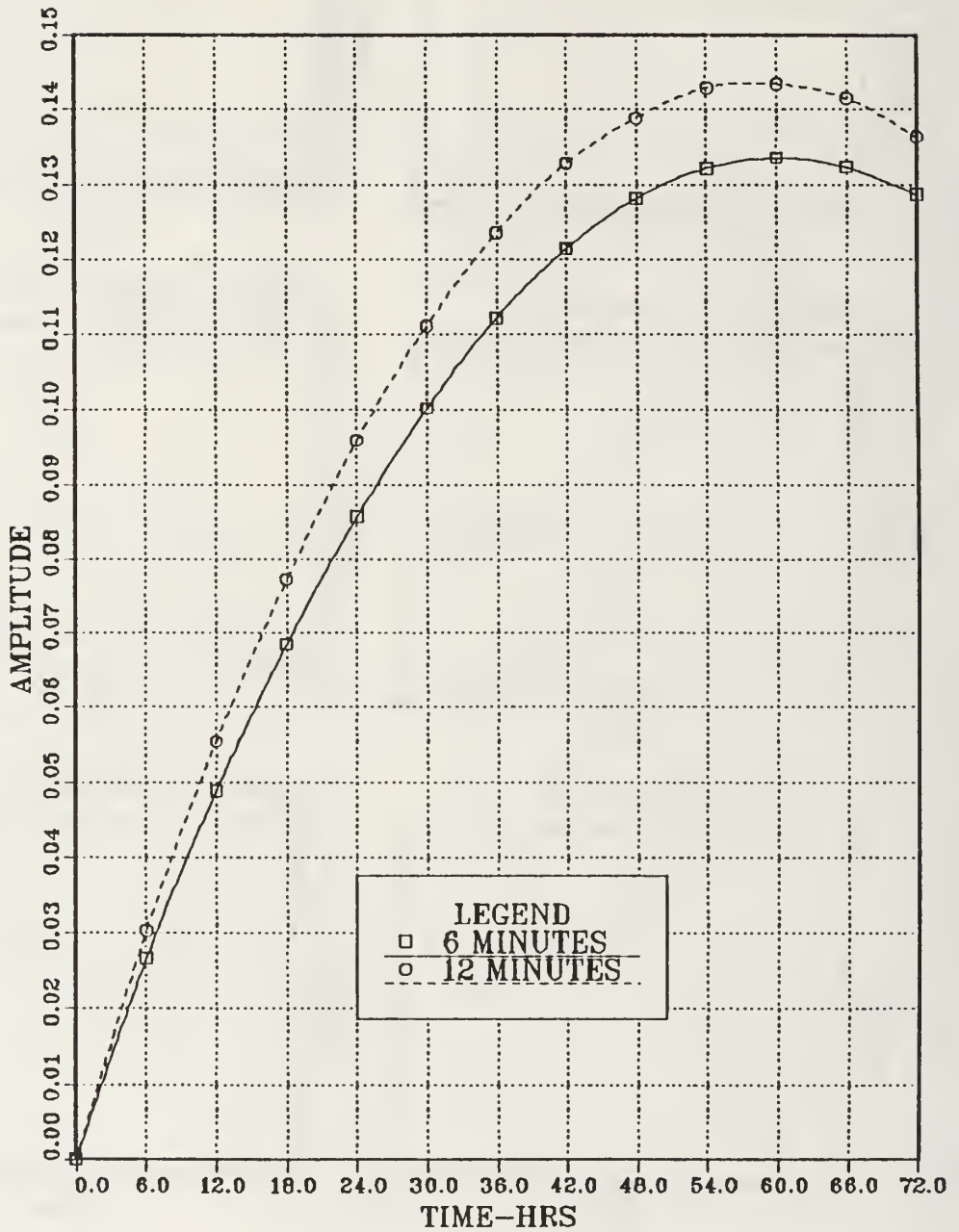


Figure 18. Wave Number One Amplitude Comparison: Comparison between Semi-Lagrangian Model run at a time step of 6 min and a time step of 12 min

V. CONCLUSION

During this research, a model was developed to see if the semi-Lagrangian method is practical on a regional scale for use in forecasting the movement of tropical cyclones. Throughout this research, we compared the results to a finite difference model used in previous research to study different effects on the movement of tropical systems.

In Chapter III of this study, we looked at how the model performed in a basic state with a mean flow from the east, no beta term was included. In this case at comparable time steps and grid intervals, both models performed well. The exception was the steadiness observed with the semi-Lagrangian model forecast track. The semi-Lagrangian model was more consistent in both speed and direction. As expected, as we increased the time step, the semi-Lagrangian model gave a better forecast. Yet, the large time steps seen in other research were not possible due to the curvature and shear of the flow near the storm center. The largest time step practical in this study was six times the largest time step possible in the finite difference model. Though between two and three times the maximum time step of the finite difference model, the number of iterations to find the displacement grew rapidly. This resulted in little improvement in CPU time efficiency as the time step was lengthened. When varying the resolution, experiments proved that the semi-Lagrangian model gives good phase speed and is not hampered by computational dispersion as seen in the finite difference model. Though, it was seen that the magnitude of the fields in the early forecast periods of the semi-Lagrangian model at coarser grids was much lower than that of the finite difference model. The amount of damping experienced was more a function of the grid interval than the time interval.

In this model, the accuracy of the displacement during the iteration step was determined to be very important in regards to the accuracy of the forecast, becoming more significant when the time step was increased. The number of iterations required to meet a certain error restriction rapidly increased as the time step increased which caused the computer run time to increase significantly. Thus as we increased the time step, no savings in computer resources were experienced.

In Chapter IV, we looked at how this model handled the movement of the vortex on a beta plane. To isolate the beta effect, we left out the mean flow. The results of our research followed that of previous work. The general track of the vortex went to the

northwest. Changing time step and grid size, caused changes in the forecast parameters specifically the component wind fields. This is due to the different levels of damping that occurred with each of the different runs. Extending the grid interval to 80 km, demonstrated significant damping in all fields. The wind fields had speeds of 10-15 m/s less than the runs completed at 40 km. The forecast track was erratic with a more northerly drift. The overall distance traveled was also significantly shorter. In Chapter III when we varied the time step and grid interval, the forecast track was comparable in all cases. Though, in the experiments in chapter four with beta included, the forecast tracks differed from slight to significant changes in direction and speed of movement.

Changes in the time interval also produced changes in the asymmetric wave number one circulations, beta gyres. Increasing the time step, increased the amplitude of the gyre and in turn strengthened what Fiorino and Elsberry (1989) referred to as the ventilation flow between the two gyres. Increasing the resolution also changed the orientation of the gyres and the amplitude of the gyres.

In conclusion with the semi-Lagrangian model, we did not see any convergence of the forecast tracks to a "true track" as we varied the resolution as is found with the finite difference schemes. This may be related to the interpolation routine of spline fitting. Though much evidence also relates this occurrence to the strength of the component wind fields. The strength and orientation of the asymmetric gyres also corresponded directly to the changing track motion of the vortex. Though the steadiness of the track of the semi-Lagrangian is better to isolate the effects of the varying parameters and not the movements caused by mathematical calculations, one needs to ensure the track changes are not due to the scheme itself. The semi-Lagrangian scheme has some positive contributions to future study and use in tropical models. Though modifications will be required to improve the efficiency of the scheme used in this research. Also, the question of solution convergence must be re-examined.

VI. RECOMMENDATIONS

The following recommendations are made for follow on study:

- Improvements to the Model
 1. Change bicubic spline routine so as it can be applied to each point individually vice over the entire grid field to save time.
 2. Set the error restriction during the calculation of the displacement so as it is equal at each point and not a field average.
- Follow on Study
 1. What relation exists between the wind fields in the various runs at different time steps and grid intervals and how do they correspond to the observed track changes.
 2. Detail the features of the asymmetric circulation that change between iterations of the semi-Lagrangian model.

REFERENCES

- Calhoun, C. R., Capt USN (ret) 1981: *Typhoons The Other Enemy*. Naval Institute Press, ix-x.
- Chan, J. C. L., and R. T. Williams, 1987: Analytical and Numerical Studies of the Beta-Effect in Tropical Cyclone Motion. *J. Atmos. Sci.*, **44**, 1257-1265.
- Environmental Group Pacific Command, 1983: Tropical Cyclone Conference Proceeding Report. Environmental Group Pacific Command Headquarters, Commander in Chief, Pacific, Camp H.M. Smith, HI.
- Fiorino, M., and R. L. Elsberry, 1989: Some Aspects of Vortex Structure Related to Tropical Cyclone Motion. *J. Atmos. Sci.*, **46**, 975-990.
- George, G. E., and W. M. Gray, 1976: Tropical Cyclone Motion and Surrounding Parameter Relationships. *J. Appl. Meteor.*, **25**, 1252-1264.
- Haltner, G. J., and R. T. Williams, 1980: *Numerical Prediction and Dynamic Meteorology*. John Wiley and Sons, 67, 110-120pp.
- Joint Typhoon Warning Center 1990: Annual Tropical Cyclone Report. U.S. Naval Oceanography Command Center, Joint Typhoon Warning Center, Guam, COMNAVMARIANAS, Box 17, FPO San Francisco 96630.
- Kuo, H. C., and R. T. Williams, 1989: Semi-Lagrangian Solutions to the Inviscid Burgess Equation. *Mon. Wea. Rev.*, **118**, 1278-1288.
- Nuemann, C. J., 1985: The Role of Statistical Models in the Prediction of Tropical Cyclone Motion. *Amer. Statistician*, **39**, 347-357.
- Peng, M. S., and R. T. Williams, 1990: Dynamics of Vortex Asymmetries and Their Influence on Vortex Motion on a Beta-plane. *J. Appl. Meteor.*, **47**, 1987-2003.

- Pudykiewicz, J., and A. Staniforth, 1984: Some Properties and Comparative Performance of the Semi-Lagrangian Method of Robert in the Solution of the Advection-Diffusion Equation. *Atmosphere-Ocean*, **22**, 283-308.
- Robert, A., 1981: A Stable Numerical Integration Scheme for the Primitive Meteorological Equations. *Atmosphere-Ocean*, **19**, 35-46.
- Sawyer, J. S., 1963: A Semi-Lagrangian Method of Solving the Vorticity Advection Equation. *Tellus* **15**, 336-342.
- Staniforth, A., and C. Templeton, 1986: Semi-Implicit Semi-Lagrangian Integration for a Barotropic Finite Element Model. *Mon. Wea. Rev.*, **114**, 95-107.
- Tsui, T. L., and R. J. Miller, 1988: Evaluation of Western North Pacific Tropical Cyclone Objective Forecast Aids. *Wea. and For.*, **3**, 76-85.
- Tupaz, J., 1977: A Numerical Study of Barotropic Instability of a Zonally Varying Easterly Jet. Dept of Meteorology, Naval Postgraduate School, Monterey, CA 93940.

INITIAL DISTRIBUTION LIST

	No. Copies
1. Defense Technical Information Center Cameron Station Alexandria, VA 22304-6145	2
2. Library, Code 52 Naval Postgraduate School Monterey, CA 93943-5002	2
3. Chairman (Code MR/Hy) Department of Meteorology Naval Postgraduate School Monterey, CA 93943-5000	1
4. Professor Roger T. Williams (Code MR/Wu) Department of Meteorology Naval Postgraduate School Monterey, CA 93943-5000	2
5. Professor Melinda S. Peng (code MR/Pg) Department of Meteorology Naval Postgraduate School Monterey, CA 93943-5000	1
6. LT Teri Ann Lentz W238 N6311 Pembroke ST Sussex, WI 53089	1
7. Commander Naval Oceanography Command Stennis Space Center MS 39529-5000	1
8. Commanding Officer Fleet Numerical Oceanography Center Monterey, CA 93943-5005	1
9. Commanding Officer Naval Oceanographic and Atmospheric Research Laboratory Stennis Space Center MS 39529-5004	1
10. Director Naval Oceanographic and Atmospheric Research Laboratory Monterey, CA 93943-5006	1

- | | | |
|-----|--|---|
| 11. | Chief of Naval Research
800 North Quincy Street
Arlington, VA 22217 | 1 |
| 12. | Office of Naval Research
Naval Ocean Research and Development Activity
800 N. Quincy Street
Arlington, VA 22217 | 1 |

DUDLEY KNOX LIBRARY
NAVAL POSTGRADUATE SCHOOL
MONTEREY CA 93943-5101



GAYLORD S



DUDLEY KNOX LIBRARY



3 2768 00019211 6